SOILS AND FOUNDATIONS Vol. 49, No. 5, 757–775, Oct. 2009
Japanese Geotechnical Society

THE SOIL PROPERTIES OF LAKE-BOTTOM SEDIMENTS IN THE LAKE BAIKAL GAS HYDRATE PROVINCE

SATSUKI KATAOKA[i], SATOSHI YAMASHITA[ii], TAKAYUKI KAWAGUCHI[iii] and TERUYUKI SUZUKI[ii]

ABSTRACT

The purpose of this study is to understand the soil properties of grounds which contain shallow type gas hydrates. For this purpose, the surveys were conducted in Lake Baikal, Russia from 2005 to 2007, where shallow gas hydrates existed. For the lake-bottom sediments, physical and mechanical properties were tested (on-board and laboratory tests). The tested samples were retrieved from the mud volcano ground which contains the shallow gas hydrates, and reference ground at the same area. From these results, it was found that the gas hydrates distribute in large amounts in the lake-bottom sediments of Lake Baikal, and that form of the gas hydrates are varied. In addition, the reference samples in Lake Baikal have no marked differences in the soil properties of the sediments obtained from other sea-bottom grounds. On the other hands, the strengths of the mud volcano samples were lower than those of the reference samples. It would seem that these results are due to the effect of the disturbance of sedimentary layers by upwelling of gas and water from underground and the pressure release during the sampling.

Key words: gas hydrate, physical property, Lake Baikal, shear modulus, site investigation, unconfined compression strength (**IGC**: D2/D6)

INTRODUCTION

Natural gas hydrates are clathrate hydrates that form when guest gas (the main component is 'methane gas') comes into contact with water under low-temperature and high-pressure conditions. A pressure of at least 5 MPa (about 50 atm) is required for gas hydrate to be stable at a temperature of 280 K (about 7°C). Therefore, natural gas hydrates occur worldwide in marine sediments (e.g., along continental margin), in sediments of deep lakes (e.g., Lake Baikal), and in polar sediments associated with permafrost conditions (e.g., Chersky and Makogan, 1970; Stoll et al., 1971). When gas hydrate-bearing zone exists in sea- and lake-bottom, free gas zone exists below the gas hydrate zone because the ground temperature increases with depths exceeding a certain level. The boundary between the gas hydrate and free gas zones is a marked acoustic reflector that is recognized as a bottom-simulating reflector (BSR, *see* in Fig. 1). The presence of a BSR is confirmed by acoustic probe, which is used effectively in estimating the distribution of gas hydrates (Scholl and Creager, 1973).

Natural gas hydrates are classified by deposition depth as deep or shallow. Deep gas hydrates exist immediately above the BSR, which is approx. 250 m below the seafloor. They have been recovered in regions including the Nankai Trough off Japan (e.g., Matsumoto et al., 2004) and the Mackenzie Delta in Canada (e.g., Dallimore et al., 2002). Shallow gas hydrates are found in sediments of the surface layer or the exposed seafloor. They have been recovered off Sakhalin in the Okhotsk Sea (e.g., Shoji et al., 2005) and in the Gulf of Mexico (e.g., Francisca et al., 2005; Yun et al., 2006). The pattern of distribution of gas hydrate in a core sample depends on the particle size of the source sediment (Clennell et al., 1999). Deep gas hydrates, which occur in sandy soils, fill in the pore spaces in the soil, whereas shallow gas hy-

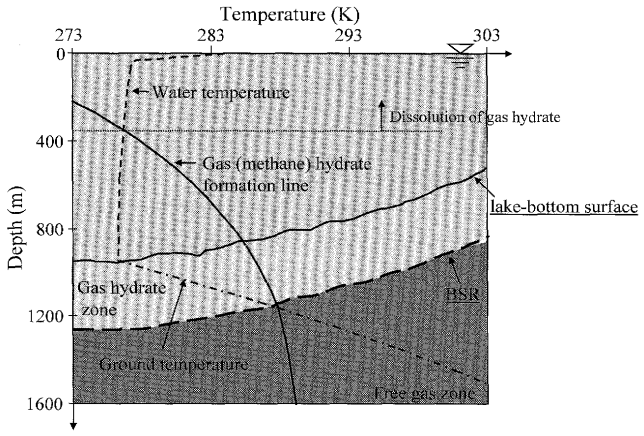

Fig. 1. Phase equilibrium diagram of gas hydrate

[i] Assistant Professor, Hakodate National College of Technology, Japan (kataoka@hakodate-ct.ac.jp).
[ii] Professor, Kitami Institute of Technology, Japan.
[iii] Associate Professor, Hakodate National College of Technology, Japan.
The manuscript for this paper was received for review on July 25, 2008; approved on July 27, 2009.
Written discussions on this paper should be submitted before May 1, 2010 to the Japanese Geotechnical Society, 4-38-2, Sengoku, Bunkyo-ku, Tokyo 112-0011, Japan. Upon request the closing date may be extended one month.

drates, which occur in silty soils, exist in clumps and veins (e.g., Bohrmann et al., 2002).

Gas hydrates are attracting attention as a next-generation energy source. Surveys and test drillings of gas hydrates for resource development have been conducted in and around the Nankai Trough and the Mackenzie Delta. Engineering studies have been under way as well. Clayton et al. (2005) prepared sandy soil samples containing gas hydrates and measured the damping and bulk modulus of the samples to analyze the seismic exploration data of gas hydrate-bearing seafloor. The sample containing gas hydrates showed higher damping than the sample without gas hydrates with the same moisture content, and the percentage of gas hydrate in the pore space was found to greatly influence the bulk modulus. Priest et al. (2005) measured the shear wave velocity of sandy soil samples with various percentages of gas hydrate in the pore space for validating theoretical models relating seismic wave propagation in marine sediments to hydrate pore saturation. They clarified that the shear wave velocity increases as the percentage of gas hydrate in the pore space increases and that the shear wave velocity is dramatically higher when the gas hydrate accounts for 3% to 5% of the total pore space, because the gas hydrates bind the gas and sand particles.

Deep gas hydrates have been studied for resource development, as stated above, and shallow gas hydrates have been attracting attention in relation to the global environment. Methane gas contained in the natural gas hydrates has approximately 20 times the greenhouse effect of CO_2. There are concerns that dissociation of methane gas, from the gas hydrates distributed in submarine surface layers, due to rising ocean temperatures or vaporization at recovery of the hydrates for energy may contribute to global warming, which in turn may raise the sea level causing climatic instability. Figure 2 shows the distribution of gas hydrates in the seas around Japan, where recovery of gas hydrate is under way, and the boundaries of tectonic plates, which are seismically active. Many gas hydrate-bearing areas are distributed near the boundaries of tectonic plates, as shown in the figure. Gas hydrates in the surface layer of seafloor may dissociate when seismic activities cause seafloor landslides that in turn cause gas hydrate-bearing layers to fail.

There have been concerns over the environmental effects of shallow gas hydrates, but surveys and samplings for shallow hydrates have been fewer than those for deep hydrates. Francisca et al. (2005) surveyed sediments on the seafloor in the Gulf of Mexico and found shallow gas hydrates on an oil-filled discontinuity plane. In addition, it is found that the sediment strength markedly decreased as a result of an increase in electrical repulsion between sediment particles when gas hydrate dissociation reduced the salinity of the pore water in the collected hydrate-bearing sediment and as a result of pore water pressure increase from vaporization of dissolved gas in the pore water. Few studies on shallow gas hydrate-bearing ground have been conducted, and the engineering studies conducted by Francisca et al. (2005) are particularly rare. To evaluate the soil properties of shallow gas hydrate-bearing sediments, it is necessary to consider secondary factors, including salinity, because salinity influences the physical and mechanical behaviour of the sediments on the seafloor such as those in the Gulf of Mexico.

In this study, we clarify the similarities and differences in physical and mechanical properties of sediments with and without gas hydrates by observation and by conducting various physical and mechanical tests on gas hydrate-bearing sediments recovered from the surface layer of the bottom of Lake Baikal in Russia, where gas hydrates exist in freshwater. Changes in mechanical properties associated with the disturbance of the sediment sample recovered from the gas hydrate-bearing ground will be clarified.

STUDY SITE

Lake Baikal (*see* in Fig. 3) is 680 km north-south by 40

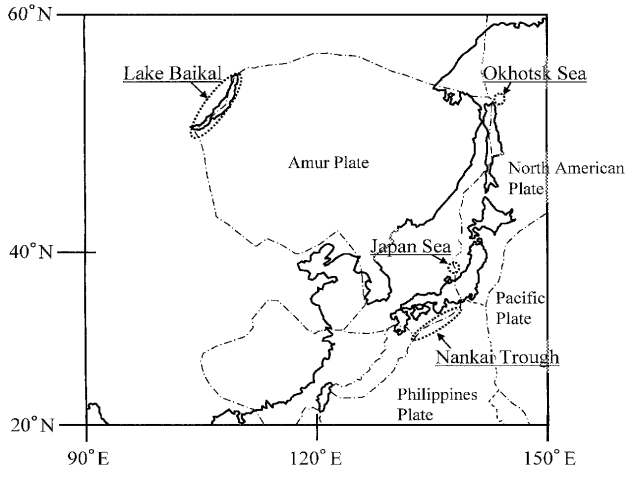

Fig. 2. Distribution of gas hydrates in the sea around Japan. In this figure, dashed lines show the plate boundary

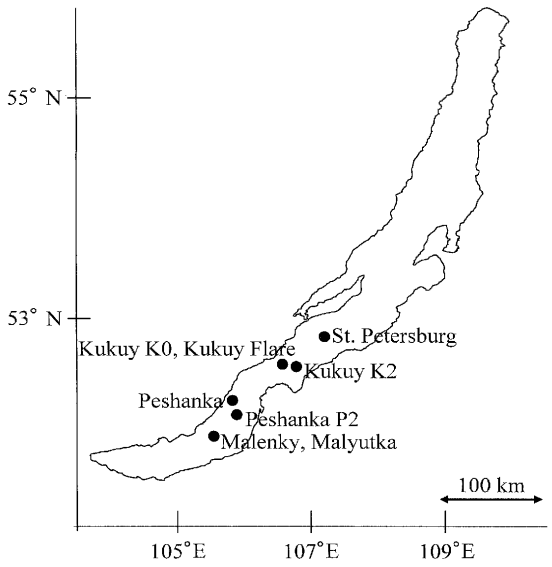

Fig. 3. The surveys sites in Lake Baikal

km to 50 km east-west (80 km maximum), and the maximum depth is 1643 m, making this lake the deepest in the world (Inoue et al., 1998). As shown in Fig. 2, Lake Baikal is on the border of Amur Plate, and there are many faults in the lake bottom. The first recovery of gas hydrates in Lake Baikal was in 1997, when the Baikal Drilling Project was conducted (Kuzmin et al., 2000), and surveys have continued in the area since then. The main studies in the Lake Baikal area have been those intended to clarify the formation and generation process of gas hydrates using water and gas in the sediments and analyzing the isotopes and compositions of the gas (e.g., Matveeva et al., 2003). No engineering studies on the mechanical properties of the shallow sediments there have been conducted.

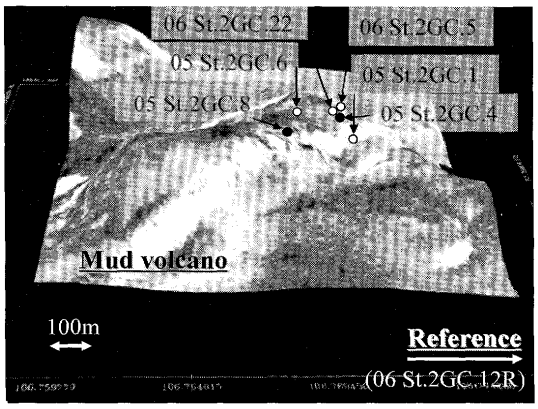

Fig. 4. 3-D bathymetric image of the mud volcano ground shows in the Kukuy K2 area (Kida et al., 2006) Symbols: open circles show the sampling area retrieved with gas hydrate cores; filled circles show the sampling area retrieved without gas hydrate cores

SURVEY AND SAMPLING STRATEGY

This paper uses samples from a survey of Lake Baikal conducted from 2005 to 2007 by the survey ship '*Vereshchagin*', owned by the Russian Limnological Institute. Core samples were collected in eight areas at the southern parts of the lake. For their proximity, the current study combines the Kukuy K0 and Kukuy Flare areas into one, and the Malenky and Malyutka areas into one. These and four other areas were surveyed, for a total of six areas (*see* in Fig. 3: solid circles). The northernmost area, at St. Petersburg, is about 160 km from the southernmost area, at Malenky-Malyutka.

It is reported that in Lake Baikal gas hydrates exist in the lake-bottom surface layer where mud volcanoes formed from the eruption of cool spring water containing gas and sediment (Matveeva et al., 2003). Acoustic probe has confirmed that gas is ejected from the lake bottom into the lake water in areas where mud volcanoes exist. To collect core samples from the hydrate-bearing soil in the present study, the lake-bottom was first explored using reflection seismology to determine the locations of mud volcanoes and to obtain seismic profiles. At locations where mud volcanoes were confirmed, shallow gas hydrate and surface sediment core samples were collected using two types of gravity core samplers. The core samplers have an outer diameter of 12.5 cm. The lengths of the samplers are 5 m and 3.5 m. Both samplers were adjusted to 700 kg by attaching dead-weights on top. They are double-pipe samplers with an inner cylindrical pipe made of vinyl chloride and having an inner diameter of 10.4 cm. The locations of core collection were determined from the echosounder images. The core sampler was lowered into the lake bottom by winch to between 10 cm and 20 cm after which it was let to freefall. After recovering, on the board, the cores for on-board tests were cut into 1 m to 2 m long sections, and each section was longitudinally halved for visual observation and testing. On-board tests were performed on a section of a clump of gas hydrate in the core. In addition, gas hydrates start on dissolving and vaporizing at water depths over about 400 m (*see* in Fig. 1) and cores recovered from the lake-bottom were left for about 2 hour in the room temperature condition on the board. Hence all small gas hydrates in the test section were almost changed to gas and water. The cores for testing at institute laboratories were kept in a sampler pipe that was stored vertically on the ship for several days, and then cut into 50 cm-long sections. Both ends of the cut pipe were sealed with paraffin for transportation.

Figure 4 shows the core sampling locations on the mud volcano in the Kukuy K2 area (Kida et al., 2006). As shown in the figure, the core samples were collected from several locations of each mud volcano, including at the top and on the slope. To compare the soil property, sediment including gas hydrates from Kukuy K2, Malenky-Malyutka and Peschanka P2 areas were also retrieved from the grounds for which gas hydrate has not been confirmed by acoustic exploration. In this paper, these samples are called 'reference'. The reference ground in the Kukuy K2 area is about 1.7 km from the mud volcano as shown in Fig. 4.

In these surveys, the lake-bottom sediments cores retrieved 135 samples from the mud volcano grounds, of which 121 were used for observation of the sediments on board and 14 were transported with whole cores to perform the laboratory tests. In the on-board tests performed on the mud volcano samples, gas hydrates were found in 34 samples. In addition, the reference cores retrieved 12 samples, of which 8 were used for observation of the sediments on board and 4 were transported with whole cores. Of the samples retrieved from lake-bottom grounds, core locations (latitude, longitude, water depth) and characteristics (the length of sampler and core length, and presence and absence of gas hydrates) of 41 cores on which on-board and laboratory tests were performed, are shown in Table 1.

TEST METHOD

On-board Tests

To measure the strength of the soil sediments immediately after recovery, the following tests were performed on-board: vane shear strength test, cone penetration test

Table 1. Core locations and characteristics

Core number	Latitude (N)	Longitude (E)	Water depth (m)	Sampler length (m)	Core length (m)	Gas hydrate
Kukuy K2						
05 St.2GC.1	52°35.358′	106°46.282′	930.0	3.5	1.35	·
05 St.2GC.4	52°35.384′	106°46.229′	938.0	3.5	2.98	
05 St.2GC.6	52°35.385′	106°46.131′	938.0	3.5	2.52	·
05 St.2GC.8	52°35.353′	106°46.120′	934.0	3.5	1.40	
06 St.2GC.5	52°35.469′	106°46.277′	908.4	5.0	2.72	·
06 St.2GC.22	52°35.461′	106°46.245′	908.4	5.0	3.00	·
06 St.2GC.12R	52°35.918′	106°46.513′	986.9	5.0	3.15	
Kukuy K0, Kukuy Flare						
06 St.6GC.1	52°30.154′	106°36.667′	427.2	5.0	4.00	·
06 St.1GC.1	52°30.342′	106°35.275′	513.6	5.0	3.24	
Malenky-Malyutka						
05 St.3GC.1	51°55.219′	105°38.104′	1370.0	5.0	1.26	·
05 St.3GC.2	51°55.217′	105°38.078′	1375.0	5.0	1.80	·
06 St.7GC.1	51°54.437′	105°36.201′	1346.3	5.0	2.17	·
07 St.1GC.4	51°55.218′	105°38.112′	1302.5	5.0	2.53	·
07 St.1GC.5	51°55.144′	105°38.148′	1289.2	5.0	0.84	·
07 St.1GC.7	51°55.161′	105°38.148′	1289.2	5.0	2.65	·
06 St.5GC.1R	51°53.312′	105°39.896′	1374.8	5.0	2.80	
07 St.10GC.2R	51°53.303′	105°39.786′	1330.0	5.0	1.69	
St. Petersburg						
06 St.3GC.2	52°52.795′	107°09.352′	1432.9	5.0	4.38	
*P*eschanka						
06 St.4GC.1	52°15.036′	105°46.519′	957.5	5.0	4.60	
Peschanka P2						
07 St.2GC.1	51°10.432′	105°48.566′	807.5	5.0	4.40	
07 St.2GC.2	51°10.455′	105°48.563′	807.5	5.0	4.60	·
07 St.2GC.3	51°10.484′	105°48.400′	817.0	5.0	4.95	
07 St.2GC.4	51°10.408′	105°48.752′	807.5	5.0	3.56	
07 St.2GC.5	51°10.458′	105°48.532′	807.5	5.0	4.34	
07 St.2GC.7	51°10.402′	105°48.477′	813.2	5.0	3.79	
07 St.2GC.8	51°10.520′	105°48.535′	818.0	5.0	4.26	
07 St.2GC.9W	51°10.500′	105°48.580′	818.0	5.0	4.40	
07 St.2GC.10	51°10.495′	105°48.482′	813.2	5.0	4.29	
07 St.2GC.11	51°10.473′	105°48.504′	807.5	5.0	4.20	·
07 St.2GC.12	51°10.437′	105°48.506′	807.5	5.0	4.20	
07 St.2GC.13	51°10.520′	105°48.556′	840.8	5.0	3.62	
07 St.2GC.14	51°10.483′	105°48.536′	812.3	5.0	2.90	·
07 St.2GC.15	51°10.504′	105°48.549′	821.8	5.0	3.42	
07 St.2GC.16	51°10.475′	105°48.544′	812.3	5.0	3.39	
07 St.2GC.17	51°10.489′	105°48.555′	812.3	5.0	2.74	·
07 St.2GC.20	51°10.478′	105°48.534′	817.0	5.0	3.20	
07 St.2GC.21	51°10.489′	105°48.533′	812.3	5.0	3.25	
07 St.2GC.122	51°10.476′	105°48.526′	807.5	5.0	3.02	
07 St.2GC.23	51°10.506′	105°48.513′	817.0	5.0	3.94	
07 St.2GC.18R	51°10.829′	105°48.362′	902.5	5.0	4.04	
07 St.2GC.19RW	51°10.849′	105°48.357′	902.5	5.0	3.81	

R: Reference cores, W: Whole cores

using a compact soil hardness tester, unconfined compression test, and measurement of shear wave velocity by bender elements. Figure 5 shows the testing points on the cut core surface.

Vane Shear Test

The test was done by using a shear vane of 10 mm in diameter, D, and 20 mm in height, H, attached to a compact torque driver. Measurements were conducted at intervals of 10 cm in the depth direction on the core surface that was longitudinally cut in half. The maximum torque, M, was measured by rotating the torque driver while penetrating the vane in the sample. The vane shear strength, τ_v, was calculated from the following equation:

$$\tau_v = \frac{M}{\pi\left(\frac{D^2H}{2}+\frac{D^3}{6}\right)} \quad \text{(kPa)} \qquad (1)$$

Cone Penetration Test using a Soil Hardness Tester

The tester used was a compact Yamanaka Soil Hardness Tester (Yamanaka and Matsuo, 1962). The diameter, length, and apex angle of the cone were 9 mm, 20 mm, and 25 degrees, and the spring strength was 1 N/10 mm. Penetration depth was measured by applying the tip of the hardness tester to the cut core surface at intervals

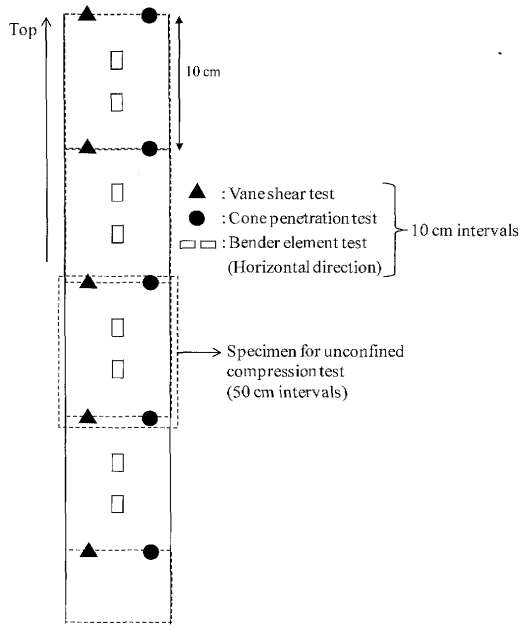

Fig. 5. Measurement location in the various on-board tests

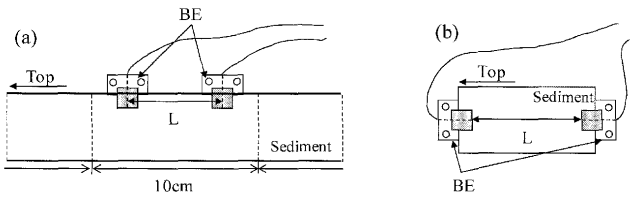

Fig. 6. On-board bender element test: (a) horizontal direction and (b) vertical direction

of 10 cm. The cone penetration resistance, q_c, was obtained using the following equation and applying the penetration strength, p, obtained from the spring strength and the sectional area of the cone, A.

$$q_c = \frac{p}{A} \quad \text{(kPa)} \tag{2}$$

Unconfined Compression Test

An unconfined compression test was done using manual loading equipment. Core samples were sectioned at 50 cm intervals in the depth direction. The resulting samples were 35 mm in diameter and 60 mm in height. Load was applied at 10 mm/min.

Shear Wave Velocity Test using Bender Elements

The setup of the bender element (BE) test is shown in Fig. 6. The BEs are inserted at 10 cm intervals on the longitudinally cut core surface and the shear wave velocity, $V_{s\text{-}1}$, is calculated from the time for the shear wave to travel between the BEs and the distance between the BEs (*see* in Fig. 6(a)). The shear wave velocity in the depth direction, $V_{s\text{-}2}$, was also determined for each unconfined compression test sample that had been cut at 50 cm intervals (*see* in Fig. 6(b)). The onboard BE test was conducted only in the 2006 survey.

Laboratory Tests

The core samples transported to the institute laboratory were subjected to unconfined compression tests done using a procedure similar to that for the on-board tests, and to incremental loading consolidation tests using test equipment with BEs (OE test), in order to understand the elastic modulus behaviour of the sample at the small strain level. The samples used in the OE test were 60 mm in diameter and 40 mm in height. Consolidation test was performed in 7 incremental loadings of 4.9, 9.8, 19.6, 39.2, 78.5, 157 and 314 kPa, and one unloading from 314 kPa to 4.9 kPa was also done. The test equipment had a pair of BEs: one at the top of the sample and the other at the bottom. At the end of each increment the shear wave velocity, V_s, was calculated and the shear modulus, G_{BE} ($=\rho_t V_s^2$), was obtained. In the equation, ρ_t is the wet density. The transmitting element was driven by ± 10 V amplitude waves from a generator with a single sinusoidal wave of different frequency. The effective propagating distance and the arrival time of the shear wave were defined by the distance from tip-to-tip of the BEs and the starting points of the input and received waves, respectively (Yamashita and Suzuki, 2001). The shear wave velocity used was the average of those measured using sinusoidal waves of 10, 15 and 20 kHz.

CORE OBSERVATION AND ONBOARD TESTS

Core Observation

Figure 7 shows soil drilling log of some of the cores retrieved in the Kukuy K2 area (*see* in Figs. 7(a) to (d)) and in the Malenky-Malyutka area (*see* in Fig. 7(e)), respectively. Photos i to v of the observed gas hydrate are for the sections shown as 1 to 5 in the stratigraphic columns. The core from the mud volcano in the Kukuy K2 area (*see* in Figs. 7(a) to (c)) consists mostly of cohesive soil, regardless of depth. These results were almost the same in the other mud volcano cores. The reference core from the Kukuy K2 area (*see* in Fig. 7(d)) consists mainly of clay layers, although clayey silt layers are present at depths of 50–65 cm and 180–200 cm. In contrast, the reference cores from the Malenky-Malyutka area (*see* in Fig. 7(e)) show alternating layers of turbidite from the depths of 40–200 cm.

In the core, spherical gas hydrate grains 0.5–1.0 cm in diameter were observed at depths of 115–126 cm (*see* in Fig. 7(a)), and directly below that area clumps of gas hydrate 5–7 cm in diameter were observed (i). In the sections deeper than 190 cm, vertically distributed gas hydrate (hereinafter: "gas hydrate plates") with thicknesses of 0.5–1.0 cm were observed (ii). Gas hydrates are observed to distribute in different patterns at different depths in the same core (*see* in Fig. 7(c)) (iv, v). In Fig. 7(b), unlike the gas hydrate observed in Figs. 7(a) and (c), gas hydrate was distributed in reticulate patterns (iii). Here, the mud volcano sample retrieved from the Kukuy K0, Kukuy Flare area also observed the vertical gas hydrate plates of more than 150 cm (*see* in Photo 1). The distribution patterns of gas hydrate are diverse even in the

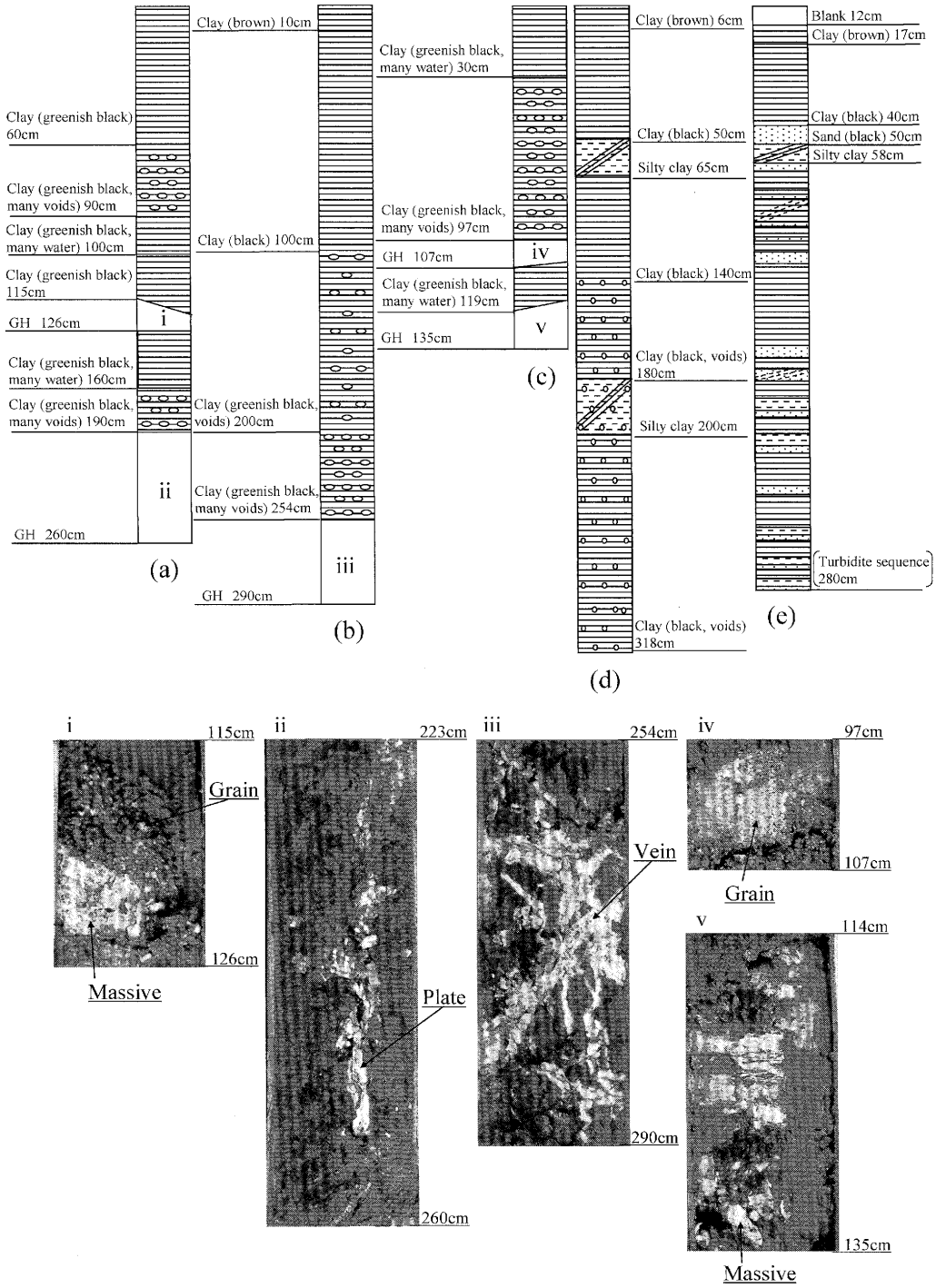

Fig. 7. Soil drilling logs and observation on natural gas hydrates. (a), (b), (c) Mud volcano samples collected from Kukuy K2 area, (d) Reference sample collected from Kukuy K2 area and (e) Reference sample collected from Malenky, Malyutka area

cores collected from a single mud volcano. The formation of various distribution patterns of gas hydrate may be attributable to the difference in particle size of the sediment around the gas hydrate and in velocities of gas and water supplied from the deeper parts of the ground (Kataoka et al., 2005). The vertical gas hydrate plate in the core, as seen in Fig. 7(a)-ii, were thought to have formed along the gas migration route in the sediment. The gas hydrate deposits in Lake Baikal were found in the clay layers similar to those found in the Sea of Okhotsk (Shoji et al., 2005), which were different in shape and deposition from the deep gas hydrate in the Nankai Trough, where gas hydrate fills the pore spaces in sandy soil. Photo 2 shows the visual observation of the cut surface of the reference sample (*see* in Photo 2(a)) and the mud volcano sample (*see* in Photo 2(b)), respectively. The depth is the same for the two cores. In Photo 2(b), many voids (from 0.1 mm to 0.5 mm in diameter) were observed in the cut surface of the mud volcano core. Here, it is known that gas hydrate formation requires

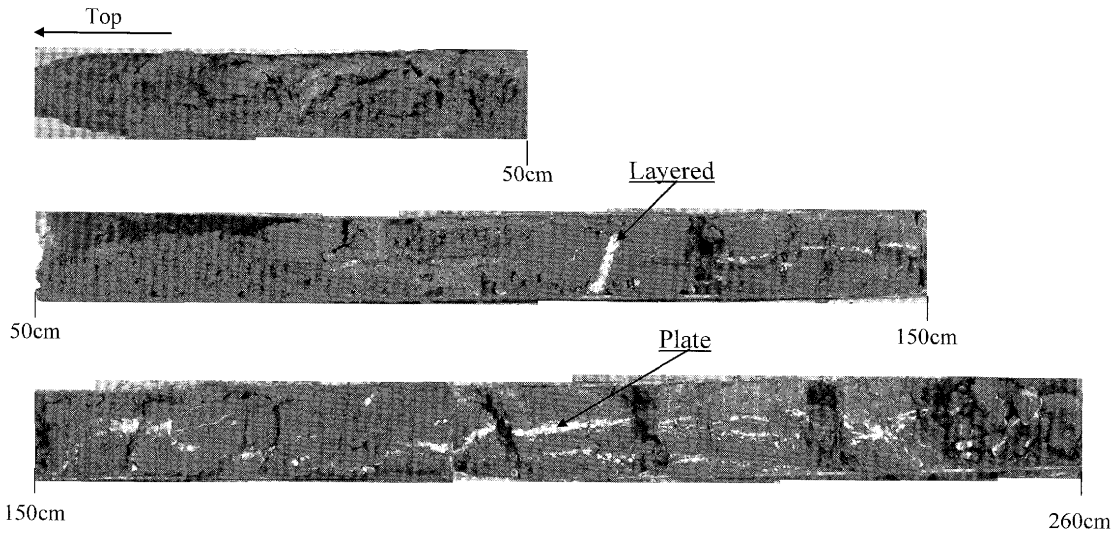

Photo 1. Core observation of sample retrieved from the Kukuy K0, Kukuy Flare area

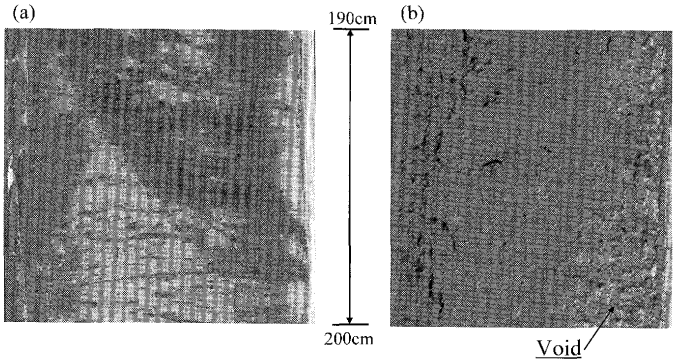

Photo 2. Observations of cut surface of cores collected from (a) reference ground and (b) mud volcano ground

that water around the gas hydrate is saturated by gas (e.g., Ohmura et al., 2004). In addition, the high pressure and low temperature are required for higher saturation ratio of gas. Therefore it would seem that the gas concentration in pore water of the mud volcano ground is likely high compared with the reference ground.

Physical Properties

Figure 8 shows grain size distribution curves for sediment samples collected in the Kukuy K2, Malenky-Malyutka, and Peschanka P2 areas. Solid lines indicate samples from mud volcanoes in each area; broken lines indicate samples from reference areas. As shown in these figures, the samples retrieved from the Malenky-Malyutka and Peschanka P2 areas have wider ranges of grain sizes than those from the Kukuy K2 area. However, the difference in grain size distribution between mud volcano and reference samples is relatively small in each area. Here, in most of the samples, diatoms of the order of 0.05–0.1 mm in maximum diameter were observed by electron microscopy (*see* in Photo 3). It is known that the sediments of Lake Baikal contain many diatoms (refer to Inoue et al., 1998). Therefore, it is considered that diatoms were sensitive to the grain size distribution.

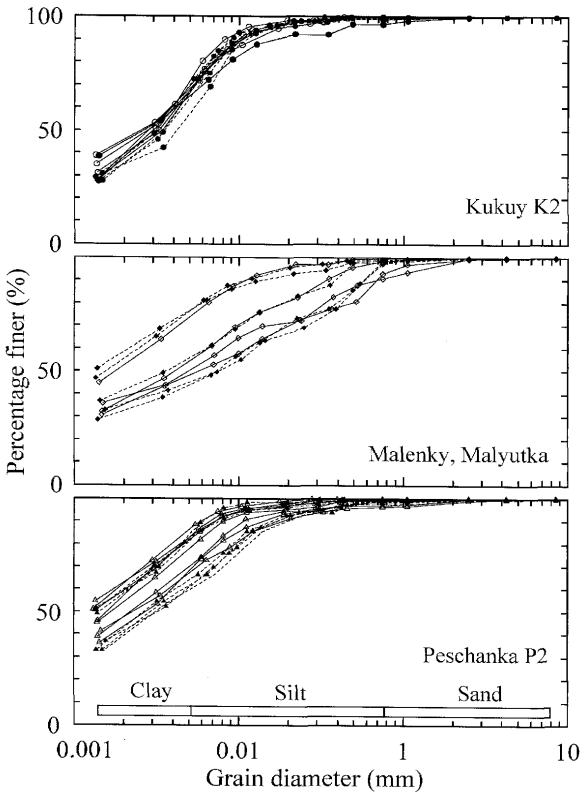

Fig. 8. Grain size distribution curves of mud volcano samples (solid lines) and reference samples (broken lines)

Figures 9, 10 and 11 show the results of the tests performed on the samples for various depths below the lake bottom using the mud volcano and reference samples retrieved from the Kukuy K2 (*see* in Fig. 9), Malenky-Malyutka (*see* in Fig. 10) and Peschanka P2 (*see* in Fig. 11) areas (a; water content, w, b; soil particle density, ρ_s, c; liquidity index, I_L, d; fines content, e; vane shear strength, τ_v, f; cone penetration resistance, q_c, g; unconfined compressive strength, q_u, and h; shear wave veloc-

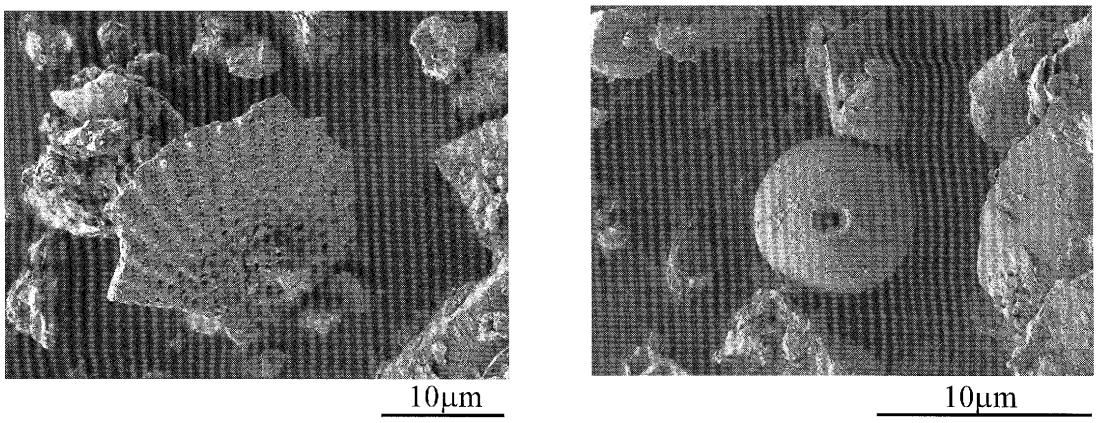

Photo 3. Diatoms observed by SEM. There were retrieved from the Kukuy K2 area (sedimentary depth; 245 cm)

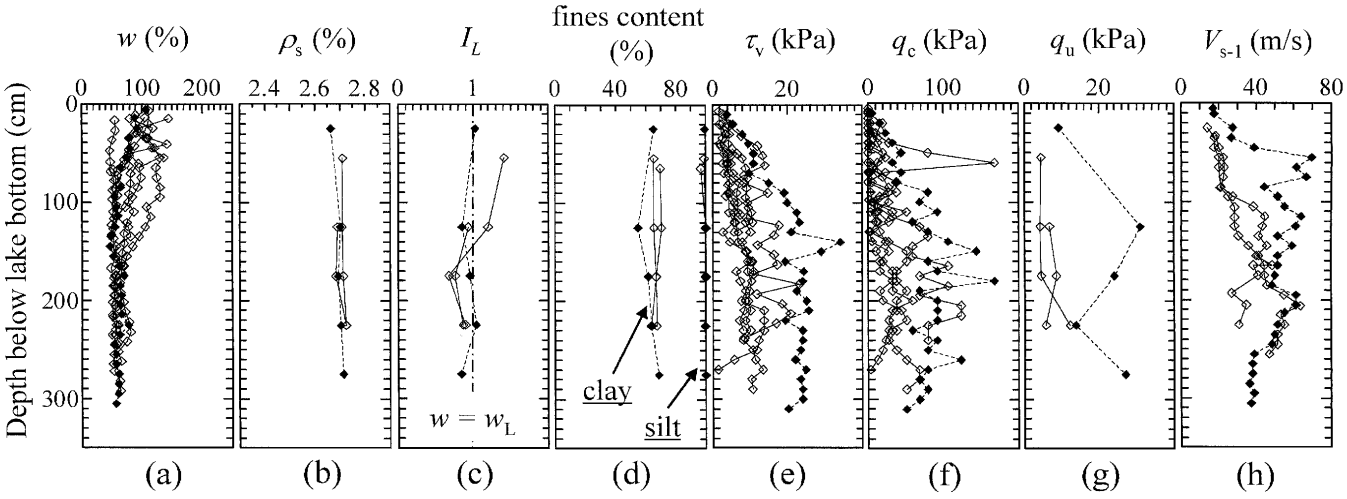

Fig. 9. Soil profiles collected from Kukuy K2 area. Symbols: filled Reference samples; open Mud volcano samples

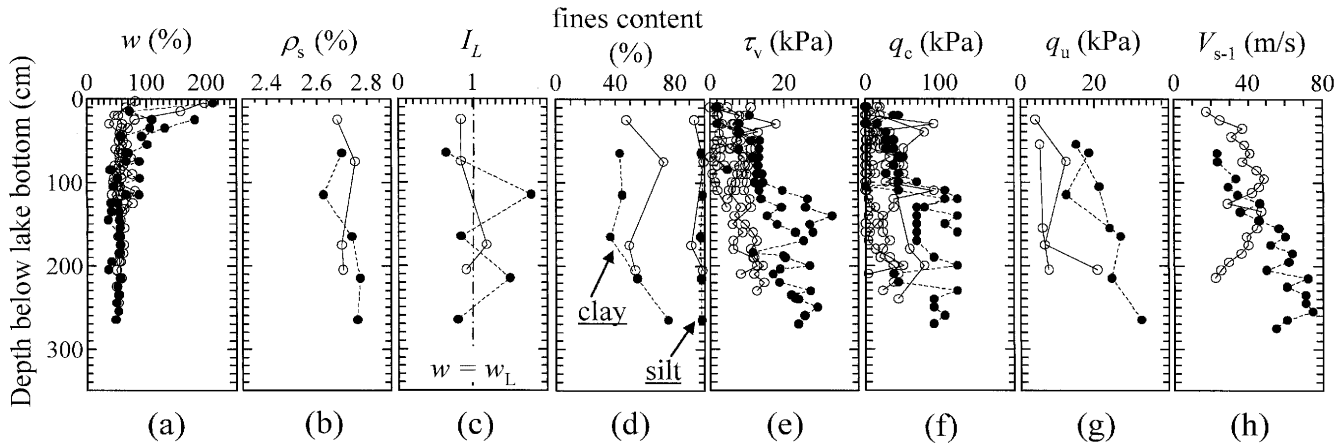

Fig. 10. Soil profiles collected from Malenky-Malyutka area. Symbols: filled Reference samples; open Mud volcano samples

ity, $V_{s\text{-}1}$). The profile of w below 150 cm of the samples in the Kukuy K2 and Malenky-Malyutka areas (*see* in Figs. 9(a), 10(a)), and below 200 cm of the samples in the Peschanka P2 area (*see* in Fig. 11(a)) are almost stable, respectively. In addition, ρ_s (*see* in Figs. 9(b), 10(b), 11(b)) except for shallow depths above 150 cm of the reference samples retrieved from the Peschanka P2 area covers a range between 2.6 g/cm^3 and 2.8 g/cm^3. As the shallow depths past above 150 cm of the reference samples retrieved from the Peschanka P2 area has a high

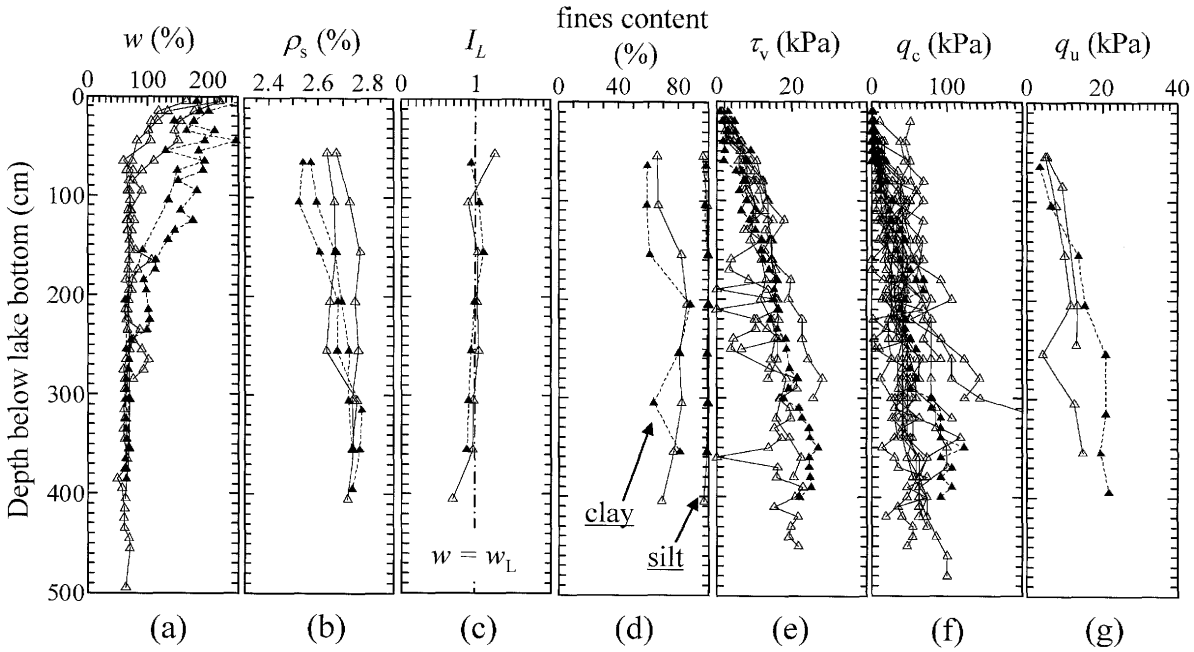

Fig. 11. Soil profiles collected from Peschanka P2 area. Symbols: filled Reference samples; open Mud volcano samples

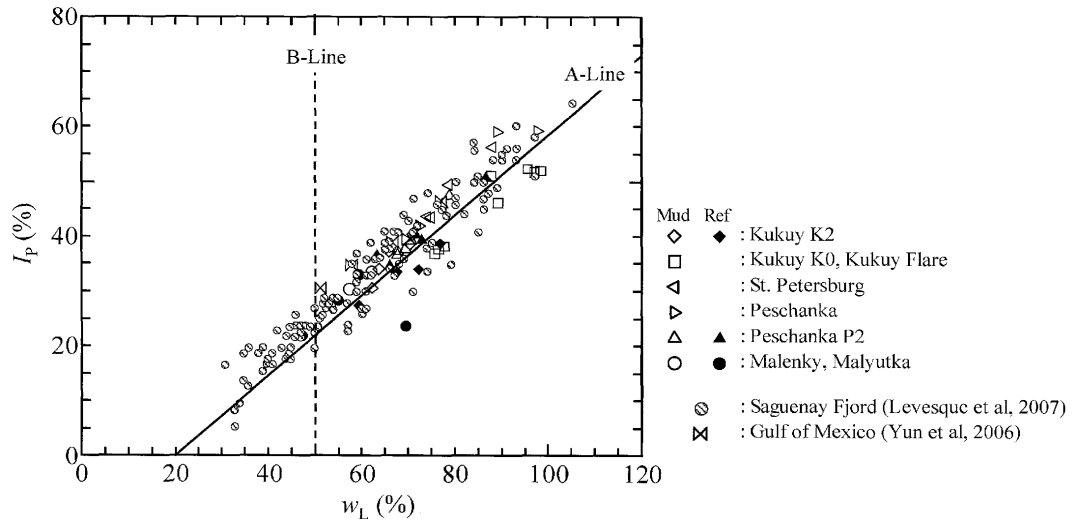

Fig. 12. Plasticity chart

value of w (between 120% and 240%) and a low value of ρ_s (between 2.5 g/cm^3 and 2.6 g/cm^3), it is considered that the diatoms and organic matter contents in this ground are possibly higher than those of other areas. I_L (*see* in Figs. 9(c), 10(c), 11(c)) except for the reference samples retrieved from the Malenky-Malyutka area show about 1.0. For the reference samples in the Malenky-Malyutka area, clay contents of depth between 0 cm and 200 cm are slightly lower than those of other areas as shown in Figs. 9(d), 10(d), and 11(d). From the soil description shown at Fig. 7(e), the reference sample retrieved from the Malenky-Malyutka area has alternate layers of clay, silt, and sand, between 50 cm and 280 cm. Therefore, it is considered that a scatter of the I_L and a decrease of the clay contents are reflected in the variation of layers.

To examine whether the sediment collected from Lake Baikal has different physical properties from those of the sediments from other aquatic gas hydrate areas, we compared the plasticity curve for the sediment from Lake Baikal with that for the sediment from the Gulf of Mexico (300 m long core collected at the water depth of 1291 m), where shallow hydrates exist (Yun et al., 2006), and with that from Saguenay Fjord in Canada (3 m to 40 m long cores collected at the water depths of 180–270 m) (Levesque et al., 2007) (*see* in Fig. 12). From Fig. 12, it is known from the mud volcano and reference samples that the sediment of Lake Baikal has a high liquid limit and that it differs little from the sediment of the Gulf of Mexico or Saguenay Fjord.

To analyze the mineral components of the sediments

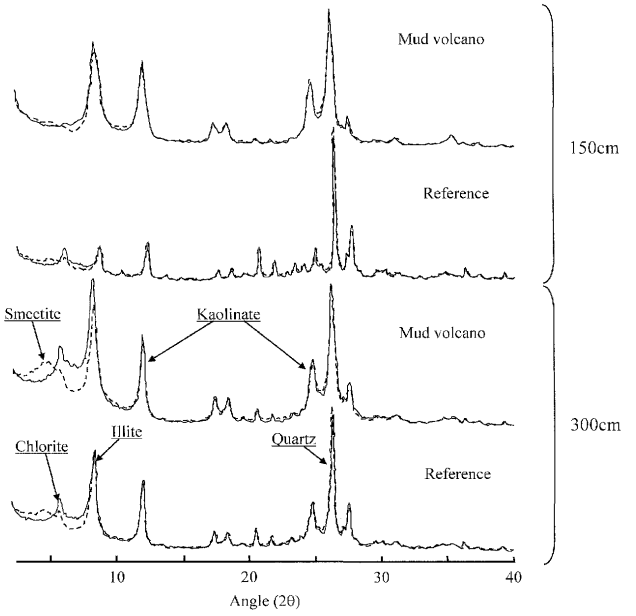

Fig. 13. X-ray diffraction of natural samples (solid lines) and glycolated samples (broken lines) of Peschanka P2 area

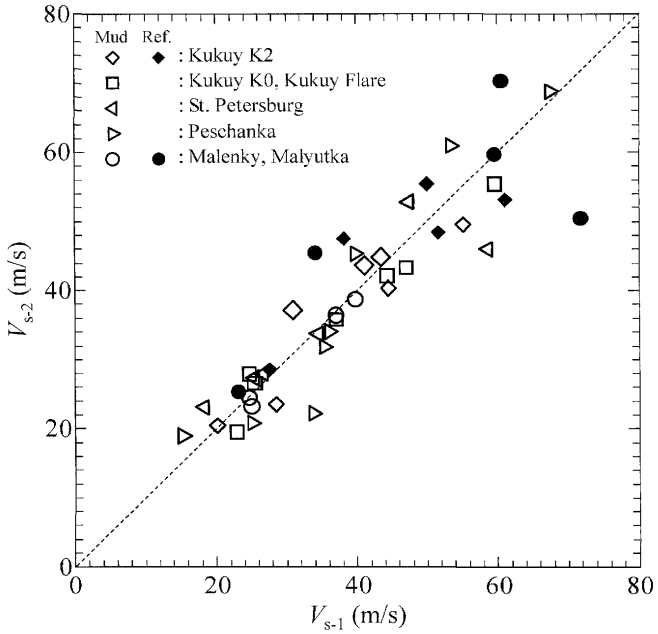

Fig. 14. Relationships of *S* wave velocity measured of horizontal direction V_{s-1} and vertical direction V_{s-2}

from Lake Baikal, an X-ray diffraction test was conducted on sediment samples from the depths of 150 cm and 300 cm in the Peschanka P2 area. At the depth of 150 cm, clay minerals such as Illite and Kaolinate were found, and at the depth of 300 cm, Smectite group minerals were found (*see* in Fig. 13), through a procedure using ethylene glycol. No clear difference was observed between the samples from the mud volcano and reference ground at any depths.

Onboard Test Results

The results of various on-board tests are also shown in Figs. 9 to 11. Here, two kinds of BE tests were performed to measure the shear wave velocity: One is done by placing the BEs horizontally to the cut core, V_{s-1} (*see* in Figs. 6(a)), and the other is done by placing the BEs vertically, at the top and bottom of the cut core, V_{s-2} (*see* in Fig. 6(b)). Compared with the results obtained from BE tests (*see* in Fig. 14), two measurements showed approximately 1:1 relationship. Therefore, it seems that the effect of the shear wave velocity on the direction of the BEs was almost nothing.

In the Kukuy K2, Malenky-Malyutka, and Peschanka P2 areas, the reference samples show higher values as the depth increases. On the other hand, the mud volcano samples retrieved from all three areas are uniformly lower than those of the reference samples. Especially, the low strengths of the mud volcano samples are remarkably observed in the unconfined compression strength, q_u. In the Kukuy K2 and Malenky-Malyutka areas, q_u of the mud volcano samples is less than half for those of the reference sample at same depth. Here, the gas concentration in pore water of the mud volcano ground is possibly higher than the reference samples retrieved from the same areas, because a gas hydrate formation requires that water around gas hydrates is saturated by gas (e.g., Ohmura et al., 2004). Additionally, it is known that the strengths of soil containing gas bubble tend to be low (e.g., Wheeler, 1988). On the basis of these reasons, it is considered that the decrease of q_u obtained from the mud volcano samples is reflected in the vaporizing of gas in pore water and the dissolving of gas hydrates by the decrease of pressure and the increase of temperature during the sampling. In addition, it should be noted in Figs. 7(d) and 9(h) that the V_{s-1} obtained from the reference sample in Kukuy K2 area is slightly high at the silty clay layers. Therefore, it seems that the difference in the strength between mud volcano and reference samples is reflected in the grain size distribution.

On evaluating the disturbance in sea-bottom sediment by evaporation of dissolved gas during sampling, it is known that the strength of the samples with gas dissolved in the pore water to saturation was approximately 25% lower than those of the samples without dissolved gas by the results of the triaxial compression tests (Lunne et al., 2001). However, the strengths of the mud volcano samples from Lake Baikal were less than half of those of the reference samples at the same depth. This is because the samples of the Lunne et al.'s test retrieved from the land sediment layer at the depth of 20 m compared with our samples were from several meters below the lake-bottom. This resulted in greater stress release in our samples; in addition, the evaporation of dissolved gas at sample recovery formed voids that temporarily increased the pore water pressure of the sample and lowered the effective stress, which in turn resulted in a strength decrease. We used an unconfined compression test in which confining pressure does not act on the sample. Our assumption for using such a test is that the disturbance at sampling has greater influence on the strength of the test samples in

our study than in the Lunne et al.'s study by used triaxial compression tests.

Comparison between the q_u of the mud volcano and reference samples from the Peschanka P2 area shows no difference in strength between the two samples from top of the core down to the depth of 200 cm. The strength of the reference sample from the Peschanka P2 area is less than those of the reference samples from the Kukuy K2 and Malenky-Malyutka areas. As shown in Fig. 11, the reference sample from the Peschanka P2 area has high w, as shown in Figs. 9(a), 10(a) and 11(a), and a low ρ_s, as shown in Figs. 9(b), 10(b) and 11(b), in the upper layer, which is attributed to the effect of diatoms and other organic matter on the strength of the reference sample. The strength of the mud volcano sediment in the sections at the depths of 200 cm or greater of the Peschanka P2 sample, similar to the samples from Kukuy K2 and Malenky-Malyutka areas, is about 50% of the strength of the reference samples, from which it is thought that the chief causes of strength decrease are disturbance of the sample by vaporization of dissolved gas, disturbance of the in-situ ground by gas and water discharge, and decrease in

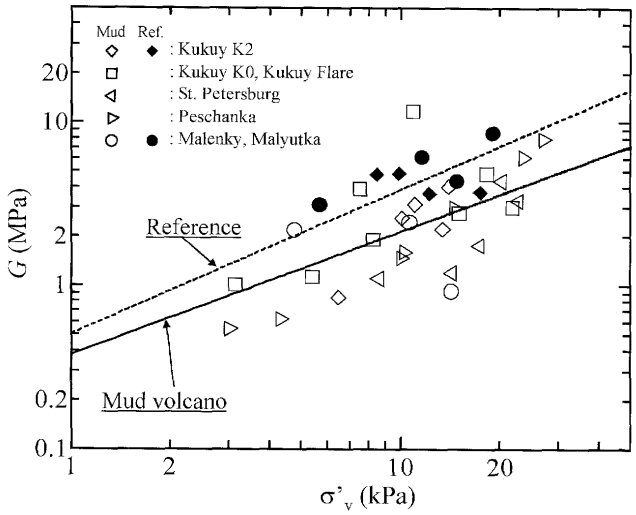

Fig. 15. Relationships between effective overburden pressure σ'_v and shear modulus G

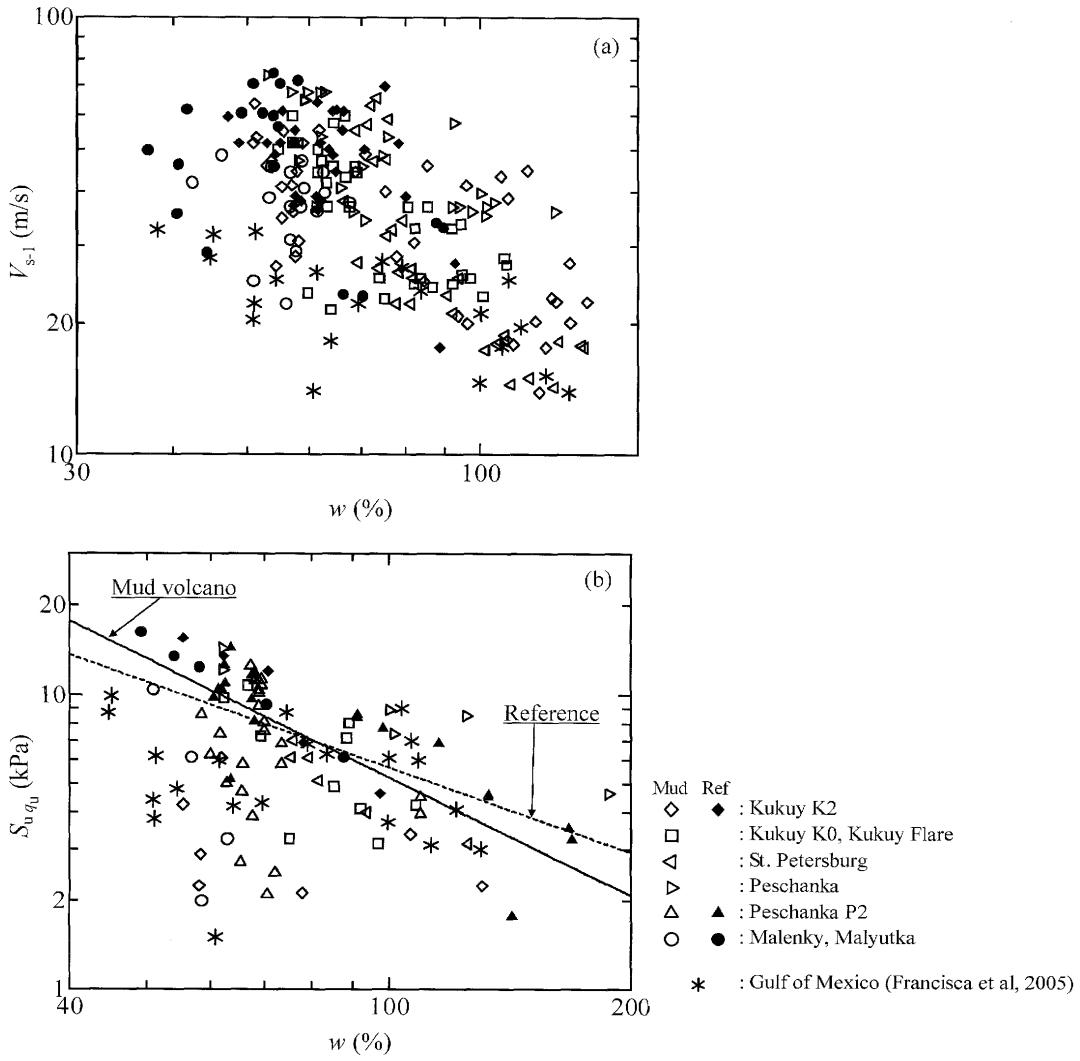

Fig. 16. Relationships between water content w and (a) shear wave velocity V_{s-1} and (b) undrained shear strength $S_{u\,qu}$

effective stress caused by increase in pore water pressure. Figure 15 shows the relationship between the shear modulus, G, obtained from the $V_{s\text{-}2}$ and the in-situ effective overburden pressure, σ'_v, of the recovered sample. From the figure, for both of the reference and mud volcano samples, the G increases with increasing σ'_v. From the approximation equation obtained from the measured values for the reference and mud volcano samples, it is found that the G tends to be lower in the reference sample (broken line: $G=0.51\sigma'^{0.88}_v$) than in the mud volcano sample (solid line: $G=0.91\sigma'^{0.75}_v$).

The relationship between the shear wave velocity and unconfined compression strength of the sediments from Lake Baikal and those of the shallow gas hydrate-bearing ground in the Gulf of Mexico was examined, and our results were compared with the values measured by Fancisca et al. (2005). Figure 16 shows the relationship between the w and the $V_{s\text{-}1}$ in Fig. 16(a), and the relationship between the w and the undrained shear strength, $S_{u\,qu}$, obtained from the q_u in Fig. 16(b). From the relationship between the w and the $V_{s\text{-}1}$, for both of the mud volcano and reference samples, when w decreases $V_{s\text{-}1}$ increases, but there is no clear difference between the values for the mud volcano and reference samples from Lake Baikal. The mud volcano and reference samples from Lake Baikal show higher shear wave velocities than those for the samples from the Gulf of Mexico at the same water content. On the other hand, in the relationship between the w and the $S_{u\,qu}$, the $S_{u\,qu}$ of the mud volcano samples are slightly lower than those of the reference samples. The undrained shear strengths of the Gulf of Mexico samples and those of the mud volcano samples from Lake Baikal are similar. Koumoto and Houlsby (2001), based on the w and the liquid limit, w_L, expressed the undrained shear strength of the Ariake clay in the following equation:

$$S_u = 1.38 w_L^{4.61/I_{PN}} w^{-4.61/I_{PN}} \quad \text{(kPa)} \qquad (3)$$

Where, $I_{PN}=\ln w_L - \ln w_P$. By substituting the w_L and the w_P obtained from the mud volcano and reference samples from Lake Baikal into the Koumoto and Houlsby equation we obtained the $S_{u\,qu}$. The resulting approximation lines are shown in Fig. 16(b). The I_{PN} of the mud volcano sample is 0.78, and that of the reference sample is 0.96. The measured values for the mud volcano samples are farther from the mud volcano approximation line (solid line) than the measured values for the reference samples are from the reference approximation line (broken line), which suggests that the mud volcano sample underwent greater disturbance than the reference sample did.

Comparison of Onboard Test Results

Figure 17 shows comparisons of the undrained shear strength between the vane shear tests, $S_{u\,\tau v}$, and the unconfined compression test, $S_{u\,qu}$, performed on the onboard. From this figure, $S_{u\,\tau v}$ and $S_{u\,qu}$ are approximately the same. Therefore, it should be noted that the vane shear test performed by a compact torque driver has no marked differences in the normal in-situ test. In addition,

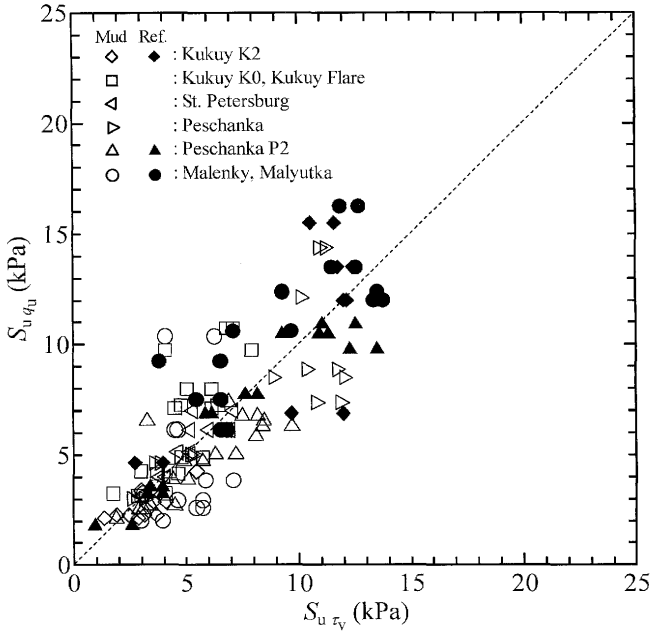

Fig. 17. Relationships of undrained shear strength calculated from vane shear test $S_{u\,\tau v}$ and unconfined compression test $S_{u\,qu}$

it is shown that the values obtained from the mud volcano samples are slightly lower than those of the reference samples.

Figure 18 shows the relationship between the q_u and q_c (*see* in Fig. 18(a)), and the τ_v and the q_c (*see* in Fig. 18(b)), respectively. The equations as shown in Fig. 18(a) ($q_c=4.87q_u$, $q_c=53+4.19q_u$) were calculated by the q_c and q_u obtained from the terrestrial clay in Japan (refer to Muromachi, 1957). In addition, the equations as shown in Fig. 18(b) ($q_c=9.74\tau_v$, $q_c=53+8.38\tau_v$) also calculated the relationship between the equation demonstrated by Muromachi (1957) (*see* in Fig. 18(a)) and '$q_u=2\tau_v$' obtained from the relation of the undrained shear strength (*see* in Fig. 17). Comparing these equations and the results obtained from on-board tests, the result obtained from on-board tests are slightly lower than the equations, respectively. Therefore, it should be noted from Fig. 17 and 18 that the q_c obtained by on-board cone penetration test is lower than the q_c obtained by normal in-situ test. It is considered that the causes for the decrease of q_c are as follows:

1) The q_c obtained from Muromachi's equations has higher and wider ranges (from 50 kPa to 800 kPa) than those of the on-board test results (from 0 kPa to 150 kPa).
2) The soil hardness tester used for the on-board cone penetration test is smaller than that of the normal in-site test.

Core Recovery Rate

As mentioned above, it is considered that a decrease of the strength and share wave velocity obtained from the mud volcano samples are reflected in the vaporization of gas contained in the pore water and the dissolution of

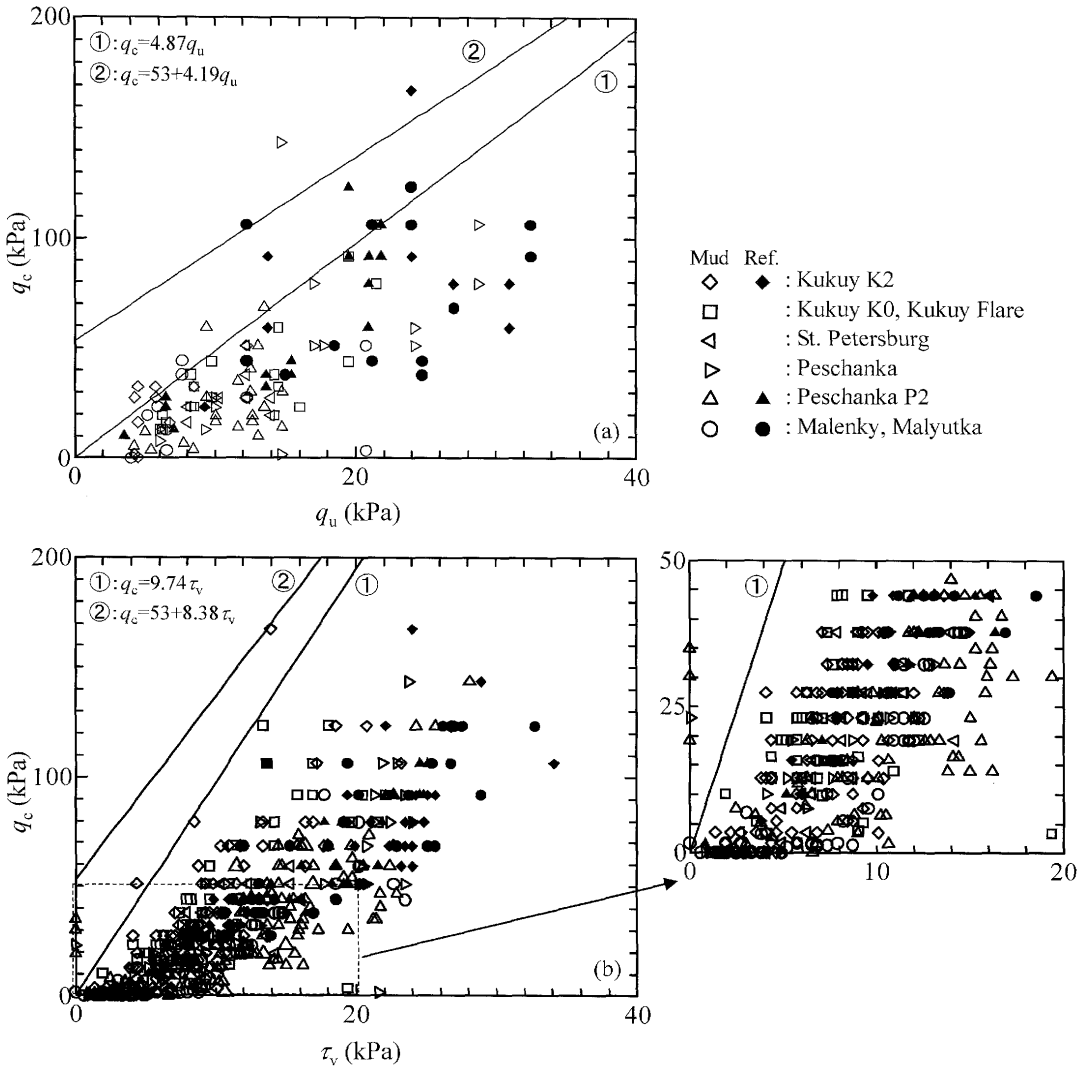

Fig. 18. Relationships between (a) the q_u and q_c and (b) the τ_v and q_c

small gas hydrates because of decrease in the pressure and increase of the temperature during the sampling. In addition, they are also reflected in the grain size distribution shown by the relationship between the soil description (*see* in Fig. 7) and the results of the soil profiles (*see* in Figs. 9 to 11). On the other hand, as shown in Fig. 7 and Photo 2, the mud volcano samples lack of a clear sediment layer compared to the reference samples. Therefore, it is considered that the strength and shear wave velocity of the mud volcano ground are possibly lower than those of the reference ground, because the mud volcano ground is disturbed by the emission of water and gas. Here, as a measure of the ground strength, Figs. 19(a) and (b) show the core recovery rate calculated by dividing the length of the core sample by the core length. In the figures, only unoccupied gas hydrates in the mud volcano cores are noted to compare with the reference cores. At the Kukuy K2 area (*see* in Fig. 19(a)), the average of the core recovery rate obtained from the mud volcano cores (72.3%) is slightly higher than that of the reference cores (66.7%). Therefore, it is supposed that the lake-bottom condition in the mud volcano ground is possibly softer

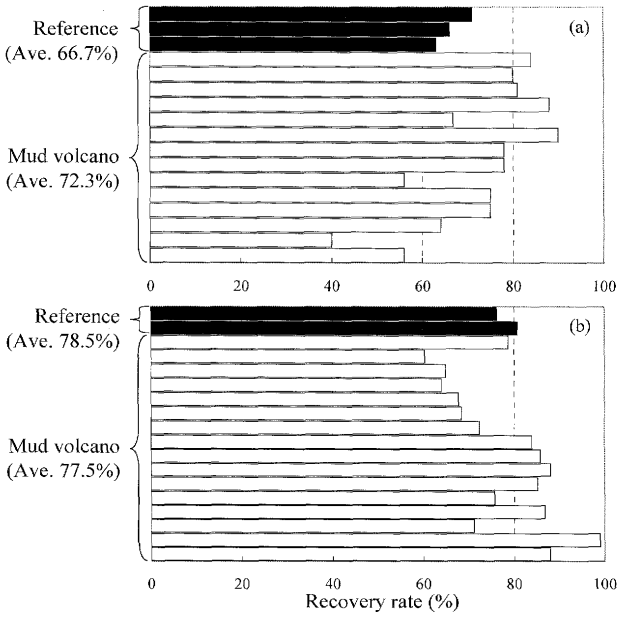

Fig. 19. Sampler penetration length at (a) Kukuy K2 area and (b) Peschanka P2 area

than the reference ground, because the mud volcano ground is disturbed by the emission of water and gas. On the other hand, the Peschanka P2 area (*see* in Fig. 19(b)) shows high values at both grounds. From this result, it is considered that the strength of grounds in Peschanka P2 area is low throughout the area, and the decrease of the mud volcano samples in this area are mainly reflected in the disturbance of the samples by the vaporization of gas contained in the pore water and the dissolution of small gas hydrates.

Therefore, from these on-board tests results, it is suggested that the strength of the sea- and lake-bottom grounds above gas hydrate are remarkably low if the decrease in the pressure and increase of the temperature occur at the sea- and lake-bottom.

LABORATORY TEST RESULTS

For the mud volcano sample immediately after recovery, the strength was lower than that of the reference sample because the mud volcano sample was disturbed by vaporization of dissolved gas at the sampling and by gas that had been discharged from the deeper part of the ground. To evaluate the mechanical properties of the mud volcano and reference samples after gas venting and recompression, we conducted unconfined compression tests and OE tests on the transported samples, and compared the unconfined compression strength and consolidation characteristics of the samples. We conducted a BE test after finishing the consolidation process of each OE test, and clarified the relationship between the consolidation pressure and the shear modulus obtained from each sample.

Unconfined Compression Test

The q_u of the mud volcano and reference samples transported from the Peschanka P2 area and that of the transported samples after remolding, q_{ur}, are shown in Fig. 20(a). We compared the strength of samples at each depth by using the figure showing the results of the onboard test immediately after sample recovery and the results of the laboratory tests after transportation. We recovered two samples from each of the mud volcano and reference locations in each area, and prepared one sample for onboard testing and one for laboratory testing.

The values for q_u of the reference samples transported and tested in the laboratory showed no marked difference from those of the reference samples tested on board. For the mud volcano samples, the q_u, which is low in the onboard test, shows values as high as those of the reference sample in the laboratory test. The q_u of the remolded sample shows a uniform value of $q_{ur} \approx 5.0$ kPa for both the mud volcano and reference samples in the onboard and laboratory tests. The sensitivity ratio S_t ($=q_u/q_{ur}$) is shown in Fig. 20(b). In the on-board test, the sensitivity ratios of the mud volcano samples are uniformly lower than those of the reference samples, which show that the mud volcano samples immediately after recovery underwent greater disturbance than the reference samples did. Even though the S_t of the mud volcano sample tested in the laboratory shows low values from the top to the depth of 150 cm, the S_t of the mud volcano sample shows higher values than that of the reference sample at the points past 150 cm and deeper. The strength of the mud volcano sample at laboratory testing is different from that immediately after recovery. From these results, it should be noted that the strength of the mud volcano samples obtained from the laboratory tests after transportation is higher than those of the on-board tests. Therefore, it is considered that the effective stress of the mud volcano samples after transportation increased compared to the on-board samples. Due to this reason, the pore water pressure, which temporarily rose because of vaporization of dissolved gas in the stress release at sampling,

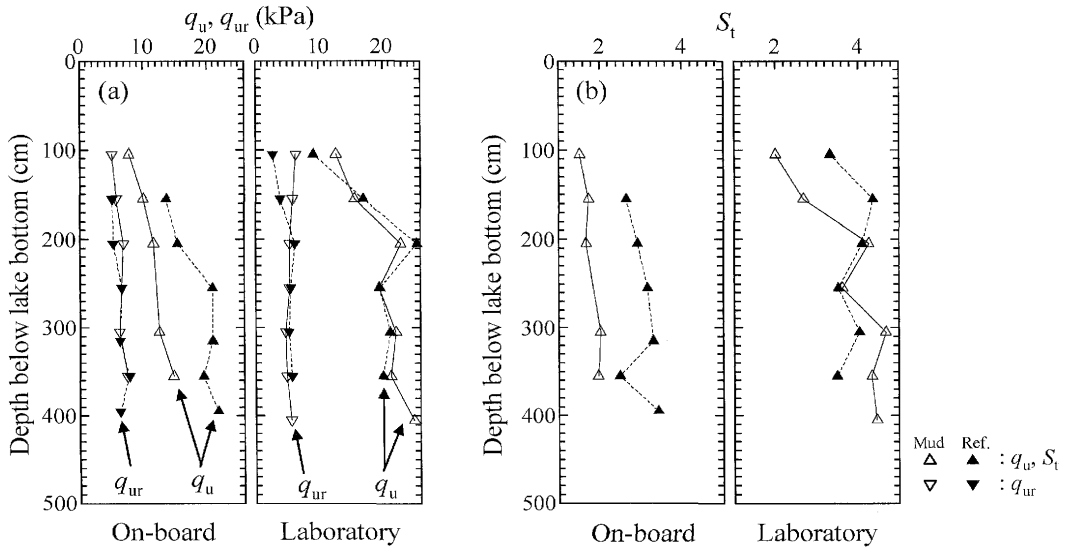

Fig. 20. (a) Unconfined compression strength profiles of undisturbed specimens q_u and remolding specimens q_{ur} measured at On-board and Laboratory tests and (b) sensitivity ratio S_t profiles

decreased during the time when sample was kept vertical for some time on board. In addition, the samples are compressed by self-weight of sediments while these were stored vertically on bored for several days, because of water drains from between the pipe and the samples. For the mud volcano samples, vaporization of dissolved gas creates voids in the core, which contribute to the greater compression in the mud volcano sample than that in the reference sample. The greater compression is thought to be one of the factors contributing to the strength increase in the transported samples.

Consolidation Test

Figure 21 shows the consolidation curves obtained from the OE test for the reference samples (*see* in Fig. 21(a)) and for the mud volcano samples (*see* in Fig. 21(b)) from the Peschanka P2 area. For the reference samples, the initial void ratio, e_0 varies from 1.8 to 2.0, and the sample recovered at the depth of 145 cm shows a high initial void ratio of $e_0 \approx 2.8$. The mud volcano samples show a uniform initial void ratio of $e_0 \approx 1.9$ at all depths. There is no depth-wise difference in the mud volcano samples. Figure 22 shows the physical properties of the samples measured in the OE tests. The w, w_L, and w_p are shown in Fig. 22(a); the ρ_s is shown in Fig. 22(b). The consolidation yield stress, p_c, obtained from Fig. 21 is shown in Fig. 22(c), compression index, C_c, is shown in Fig. 22(d), swelling index, C_s, is shown in Fig. 22(e), and coefficient of permeability, k, when the average consolidation pressures are 13.9 kPa and 111 kPa is shown in Fig. 22(f). The values are plotted depth-wise. It is found from these values that the mud volcano samples have less depth-wise variation than the reference samples have. The relationship between the p_c of the mud volcano and reference samples and the in-situ effective overburden pressure, σ'_v, shows that all of the p_c values are greater than the σ'_v values. On the basis of these reasons, it is considered that the disturbance in sedimentary layer by the emission of gas and water, and the vaporization of dissolved gas by the stress release of the mud volcano ground are reflected in the difference of the consolidation characteristics between the mud volcano and reference samples.

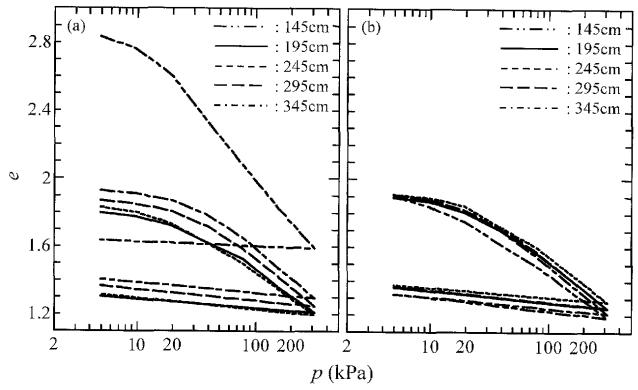

Fig. 21. Consolidation curve measured at OE test of (a) reference samples and (b) mud volcano samples collected from Peschanka P2 area

Bender Element Test

Comparison between measured q_u for the mud volcano and that for the reference samples at the large-strain region shows that the transported mud volcano and reference samples have nearly equal q_u. In this section, deformation behaviour of the transported samples at small strain region was examined from the relationship between the p at completion of consolidation process in each of the incremented OE tests and the G_{Vh} obtained from the BE test. Figure 23 shows the relationship between the p and the G_{Vh}. The σ'_v at five depths are shown in the same

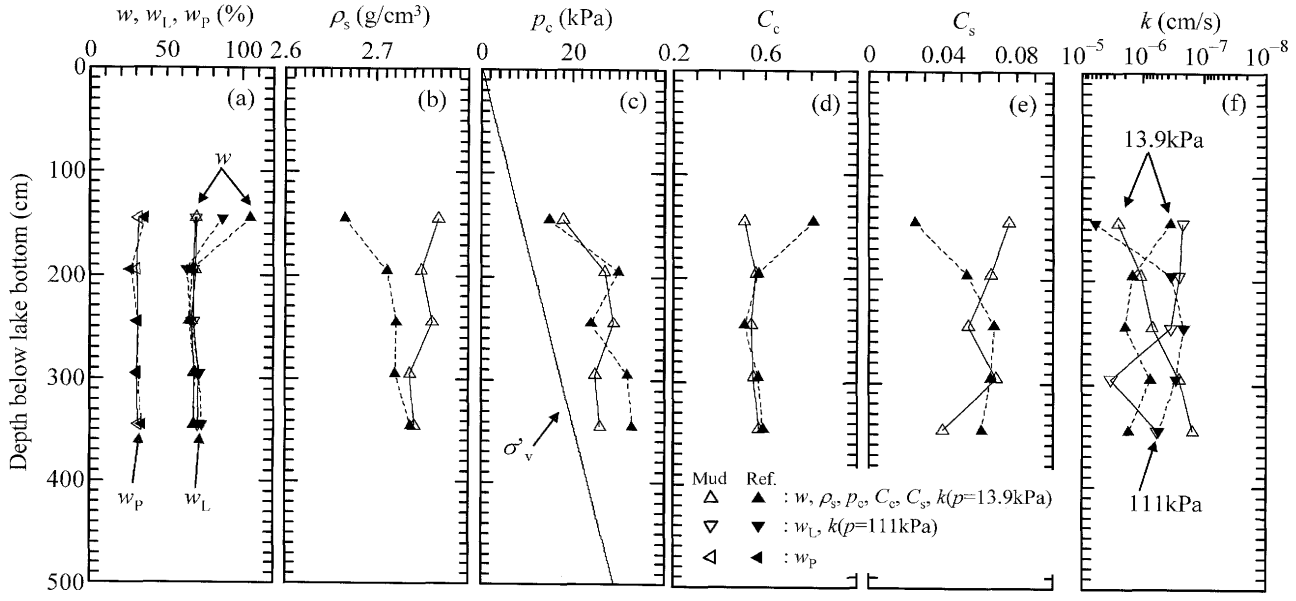

Fig. 22. Soil profiles of OE test samples collected from Peschanka P2 area

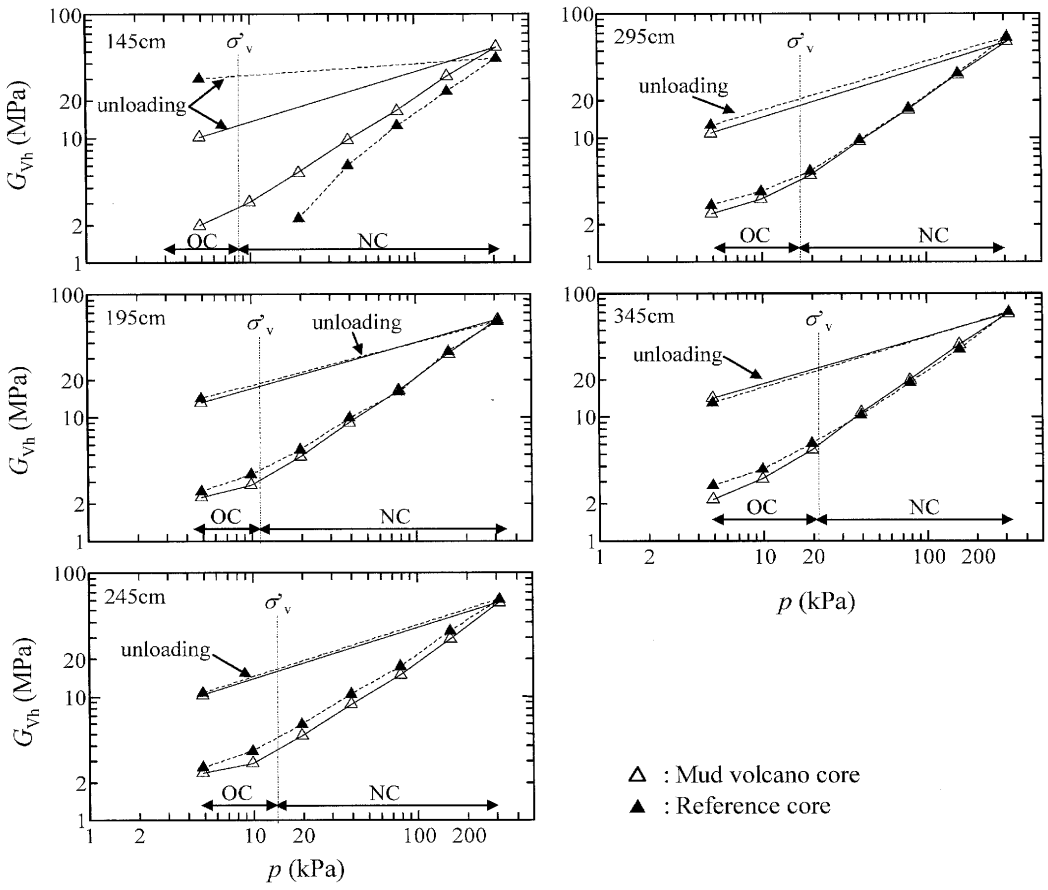

Fig. 23. Relationships between consolidation pressure p and shear modulus G_{Vh} in the Peschanka P2 area

figure. Consolidation pressure is classified in three categories: over consolidation (OC), normal consolidation (NC), and unloading. The influence of consolidation pressure on the shear modulus in each range was examined. In the OC region, the G_{Vh} of the mud volcano sample is slightly smaller than that of the reference sample. It is possible that vaporization of the dissolved gas at sampling of the mud volcano sample disturbed the sample and lowered the shear modulus, and that the sediment in the mud volcano area is disturbed by the water and gas discharge and the sedimentary structure is less developed than that of the reference ground, all of which contribute to the decrease in the shear modulus in the mud volcano samples. In the NC region, except for the reference sample at the depth of 145 cm, the difference between the shear modulus of the mud volcano and that of the reference samples decreases as the consolidation pressure increases. This is thought to be because the sedimentary structure of all samples developed uniformly with increases in the consolidation pressure. Once the sample is loaded to the NC region, the sedimentary structure does not change even if the sample is unloaded to lower than the overburden pressure, which is thought to be the reason for the approximately uniform shear modulus in the mud volcano and reference samples (*see* in Fig. 23). As for the reference sample retrieved from the depth of 145 cm, the shear modulus in the NC region is lower than those of the mud volcano sample at the same depth, because the physical properties of this sample are markedly different compared with the samples retrieved from the same area (*see* in Figs. 22(a) and (b)).

Comparison of Soil Properties between Lake Baikal and Other Sites

Compressibility of a soil is often characterized using the C_c. Logically if a soil experiences great deformations for a small change in pressure, the soil is considered to be very compressible. In natural soils, C_c can vary for different void ratios, even for sediments deposited within a single sedimentary basin (refer to Leroueil et al., 1983). Figure 24 shows the relationship between C_c and e_0 obtained from OE test, and those of the test results in Saguenay Fjord presented by Levesque et al. (2007). From this figure, there is no clear difference between the sediments of the Lake Baikal and Saguenay Fjord. Leroueil et al. (1983) demonstrated that C_c depends on the S_t and e_0. The relationship between C_c and S_t is shown by a series of lines in Fig. 24. As can be seen in Fig. 24, S_t obtained from the Lake Baikal sediments are between 1 and 4. S_t obtained from unconfined compression test tend to between 2 and 4, indicating that it is approximately possible to estimate the S_t for the OE test. The relationship between the C_c and w_L is shown in Fig. 25. In the figure, the lines obtained from equations proposed by

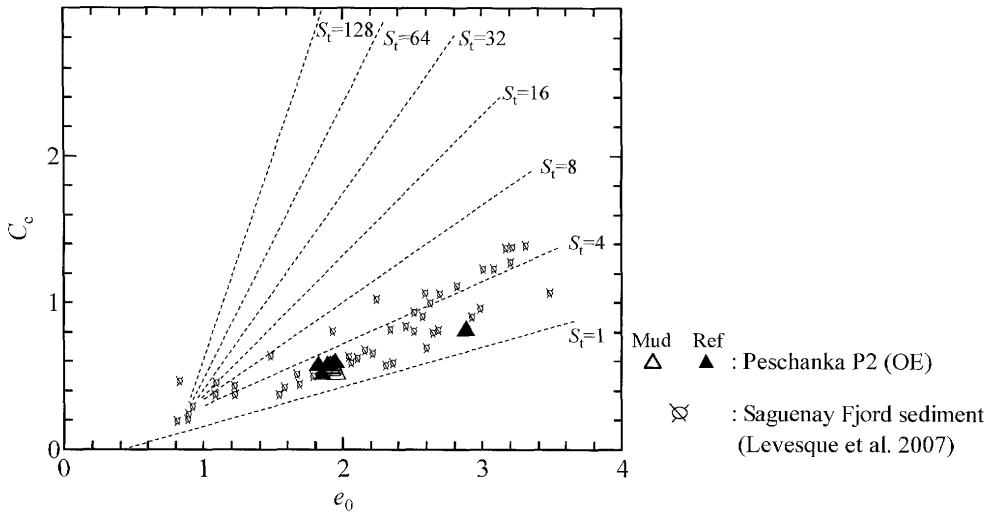

Fig. 24. Relationships between initial void ratio e_0 and compression index C_c (Leroueil et al., 1983)

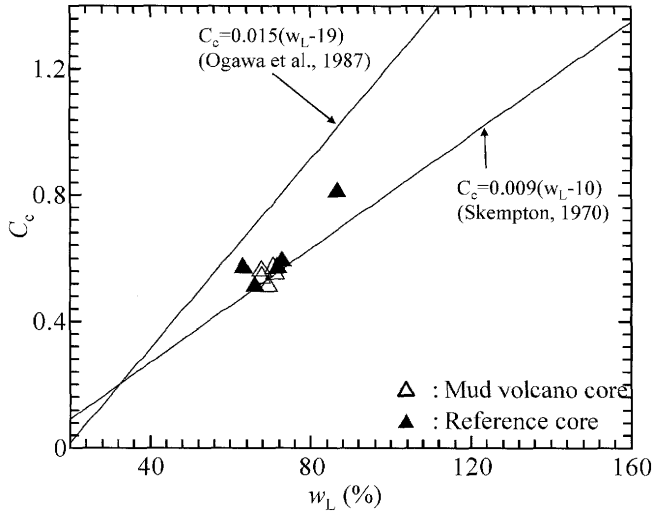

Fig. 25. Relationships between liquid limit w_L and compression index C_c

Skempton (1970) and Ogawa et al. (1987) were added to examine the relationship between the values for the Lake Baikal samples and the values obtained by the equations. It is found that the values for the Lake Baikal samples distribute near the line proposed by Skempton.

$$C_c = 0.009(w_L - 10) \quad \text{(Skempton, 1970)} \qquad (4)$$

$$C_c = 0.015(w_L - 19) \quad \text{(Ogawa et al., 1987)} \qquad (5)$$

For shear modulus, estimation equations that express the shear modulus, G_{max}, of two different types of cohesive soil as functions of the void ratio, e, have been proposed (e.g., Hardin and Black, 1969; Shibuya and Tanaka, 1996).

$$G_{max} = 3270 \frac{(2.973 - e)^2}{1 + e} \sigma'^{0.05}_m \quad \text{(kPa)}$$

(Hardin and Black, 1969) (6)

$$G_{max} = 5000 e^{-1.5} \sigma'^{0.5}_v \quad \text{(kPa)}$$

(Shibuya and Tanaka, 1996) (7)

Zen et al. (1987) did not use the e, and proposed the following equation that expresses the shear modulus in relation to the plasticity index, I_p.

$$G_{max} = (285 - 2I_p)\sigma'_m \quad \text{(kPa) (Zen et al., 1987)} \qquad (8)$$

Figure 26 shows the measured shear modulus, $G_{Vh}^{measured}$, in the OE test at the compressive pressure of $p = 9.8$ kPa, which is below the in-situ overburden pressure; at $p =$ 78.5 kPa, which is above the in-situ overburden pressure; and at 314 kPa. The figure also shows the calculated shear modulus, $G_{max}^{calculated}$, obtained from the estimation Eqs. (6), (7), and (8). The $G_{max}^{calculated}$ in the figure were obtained by assuming a value of 0.5 for the coefficient of earth pressure at rest, K_0, in the OE test. For the low consolidation pressure in the over consolidation region ($p =$ 9.8 kPa), the values for three equations slightly differ; however, for all three consolidation regions, the calculated values tend to be 0.5–2.0 times the measured values. Almost no difference is found between the shear modulus of the mud volcano and reference samples.

In light of the above, we conclude that the compression properties and shear modulus of the shallow layer sediment of Lake Baikal do not differ very much from the soil properties of sediments from the other marine areas, and it is possible to estimate the ground strength by using the conventional estimation equations.

CONCLUSIONS

The surveys were conducted in the Lake Baikal, Russia from 2005 to 2007, and several kinds of tests were conducted for the lake-bottom sediments. Based on the comparison with the core observation and various tests results on the mud volcano and reference samples, the following conclusions were obtained;

(1) Cores with gas hydrates were retrieved from the mud volcano grounds. Gas hydrates observed in the cores appear in massive, grains or veins, and their distribution patterns differed from the distribution patterns

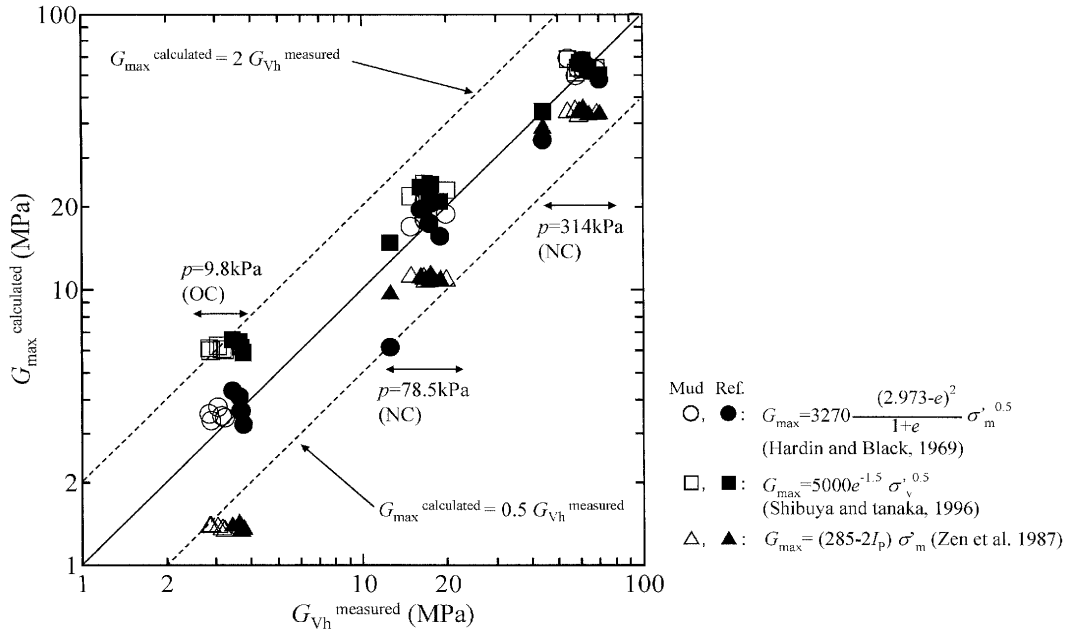

Fig. 26. Relationships between measured value G_{Vh} and calculated value by estimated equation G_{max} in the Peschanka P2 area

of deep gas hydrates, which mostly form in sandy soil.

(2) In the cores in which gas hydrates were found, many voids of 0.1–0.5 cm were observed. The voids are thought to have formed from the vaporization of dissolved gas and the dissociation of minute grains of gas hydrate associated with the temperature rise and pressure decrease during sampling.

(3) In the mud volcano samples, the clearly layered sedimentary structure that was observed in the reference sample was not observed. It is considered that the ground had been disturbed by gas discharge in the mud volcano area.

(4) Physical properties of the sediments retrieved from the mud volcano and reference grounds at the same areas were almost similar, regardless of depth.

(5) Mechanical tests conducted immediately after the sample recovery showed that the strength of the mud volcano samples was lower than that of the reference samples. From this result, it is considered that the decrease of the strength obtained from the mud volcano samples is reflected in the vaporizing of gas in pore water and the dissolving of gas hydrates by the decrease of pressure and the increase of temperature during the sampling. In addition, it also seems that the difference in the strength between the mud volcano and reference samples is reflected in the grain size distribution.

(6) When sample recovery that involves stress release is done in hydrate-bearing ground, the strength of samples immediately after recovery tends to be underestimated because of the disturbance that occurs at sampling. It is suggested that when hydrates are recovered using methods that involve temperature rise or pressure decrease, which result in dissociation of hydrates in shallow gas hydrate-bearing ground, the sea- or lake-bottom may experience reduction in stability, because of the decreased ground strength.

(7) In the sediments retrieved from the mud volcano grounds, the strengths obtained from the laboratory test were higher than those of the on-board test. Therefore, it seems like the samples were compressed by the self-weight of sediments while these were stored vertically on board for several days. On the other hand, the consolidation characteristics of the mud volcano and reference samples showed no marked differences. At small strain region, however, a moderate decrease in shear modulus was confirmed in the mud volcano samples whose consolidation pressure was lower than the in-situ overburden pressure.

From these results, it is suggested that when methane hydrates are recovered using methods that involve temperature rise or pressure decrease, which result in dissociation of methane hydrates in shallow gas hydrate-bearing ground, the sea- or lake-bottom may experience reduction in stability, because of the decreased ground strength.

ACKNOWLEDGMENTS

The authors would like to thank Dr. Mikhail Grachev and Dr. Oleg Khlystov of the Russian Limnological Institute, Dr. Jeffery Poort of Ghent University in Belgium, Dr. Hirotsugu Minami, Dr. Akihiro Hachikubo and Dr. Alexey Krylov of Kitami Institute of Technology, and Dr. Masayuki Hyodo of Yamaguchi University, Dr. Shinya Nishio and Mr. Toru Abe of Shimizu Corporation, and Mr. Tatsuya Yokoyama of Oyo Corporation for their cooperation in the surveys and tests. Thanks are also due to Mr. Keita Nanami and Mr. Yuki Konishi of Kitami Institute of Technology for their help in the physi-

cal tests after sample collection. This study was supported by KAKENHI grant #18360222.

REFERENCES

1) Bohrmann, G., Suess, E., Greinert, J., Teichert, B. and Naehr, T. (2002): Gas hydrate carbonates from Hydrate Ridge, Cascadia Convergent Margin; Indicators of near-seafloor clathrate deposits, *Proc. 4th International Conference on Gas Hydrates*, Yokohama, 102–107.
2) Chersky, N. and Makogan, Y. (1970): Solid Gas—World reserves are enormous, *Oil and Gas Invest.*, **10**(8), 82p.
3) Clayton, C. R. I., Priest, J. A. and Best, A. I. (2005): The effects of disseminated methane hydrate on the dynamic stiffness and damping of a sand, *Gèotechnique*, **55**(6), 423–434.
4) Clennell, M. B., Hovland, M., Booth, J. S., Henry, P. and Winters, W. J. (1999): Formation of natural gas hydrates in marine sediments; 1. Conceptual model of gas hydrate growth conditioned by host sediment properties, *Journal of Geophysical Research*, **104**(B10), 22985–23003.
5) Dallimore, S. R., Collett, T. S., Uchida, T., Weber, M., Takahashi, H. and the Mallik Gas Hydrate Research Team (2002): Overview of the 2002 Mallik gas hydrate production research well program, *Proc. 4th International Conference on Gas Hydrates*, Yokohama, 36–39.
6) Francisca, F., Yun, Y. S., Ruppel, C. and Santamarina, J. C. (2005): Geophysical and geotechnical properties of near-seafloor sediments in the northern Gulf of Mexico, *Earth and Planetary Science Letters*, **237**, 924–939.
7) Hardin, B. O. and Black, W. L. (1969): Vibration modulus of normally consolidated clay, *Jour. of the SMF Div., Proc. ASCE*, **95**(SM6), 1531–1537.
8) Inoue, G., Kashiwaya, K. and Minoura, K. (1998): *Science of Global Environmental Change; Baikal Drilling Project*, Kokon Shoin Co. Ltd., Tokyo, 269p.
9) Kataoka, S., Kitamura, O., Hyakutake, K., Abe, K., Hachikubo, A. and Shoji, H. (2005): Formation experiments of CO_2 hydrate chimney in a pressure cell, *Polar Meteorology and Glaciology*, (19), 42–49.
10) Kida, M., Khlystov, O., Zemskaya, T., Takahashi, N., Minami, H., Sakagami, H., Krylov, A., Hachikubo, A., Yamashita, S., Shoji, H., Poort, J. and Naudts, L. (2006): Coexistence of structure I and II gas hydrates in Lake Baikal suggesting gas sources from microbial and thermogenic origin, *Geophysical Research Letters*, **33**, L24603.
11) Koumoto, T. and Houlsby, G. T. (2001): Theory and practice of the fall cone test, *Gèotechnique*, **51**(8), 701–712.
12) Kuzmin, M. I., Karabanov, E. B., Prokopenko, A. A., Gelety, V. S., Williams, D. F. and Gvozdkov, A. N. (2000): Sedimentation processes and new age constraints on rifting stages in Lake Baikal, *Int. J. Earth Sci.*, (88), 183–192.
13) Leroueil, S., Tavenas, F. and LeBihan, J. P. (1983): Propriètès caractèristiques des argiles de l'est du Canada, *Canadian Geotechnical Journal*, **20**, 681–705.
14) Levesque, C. L., Locat, L. and Leroueil, S. (2007): Characterisation of postglacial sediments of the Saguenay Fjord, Quebec, Canada, *Characterisation and Engineering Properties of Natural Soils*, Taylor & Francis Group, London, 2645–2677.
15) Lunne, T., Berre, T., Strandvik, S., Andersen, K. H. and Tjelta, T. I. (2001): Deepwater sample disturbance due to stress relief, *NGI Rapport*, 521671–10.
16) Matsumoto, R., Tomaru, H. and Hailong, L. (2004): Detection and evaluation of gas hydrates in the eastern Nankai Trough by geochemical and geophysical methods, *Resource Geology*, **54**(1), 53–67.
17) Matveeva, T. V., Mazurenko, L. L., Soloviev, V. A., Klerkx, J., Kaulio, V. V. and Prasolov, E. M. (2003): Gas hydrate accumulation in the subsurface sediments of Lake Baikal (eastern Siberia), *Geo-Mar Letter*, **23**, 289–299.
18) Muromachi, T. (1957): The relation between cone penetration resistance and uniaxial compression strength on cohesive soils, *JSCE*, **42**(10), 7–12 (in Japanese).
19) Ogawa, T. and Matsumoto, K. (1978): Correlation of the Mechanical and Index properties of soils in Harbour Districts, *Report of the Port and Harbour Research Institute Ministry of Transport*, **17**(3), 3–89 (in Japanese).
20) Ohmura, R., Shimada, W., Uchida, T., Mori, Y. H., Takeya, S., Nagao, J., Minagawa, H., Ebinuma, T. and Narita, H. (2004): Clathrate hydrate crystal growth in liquid water saturated with a hydrate-formation substance; variations in crystal morphology, *Philosophical Magazine*, **84**(1), 1–16.
21) Priest, J. A., Best, A. I. and Clayton, C. R. I. (2005): A laboratory investigation into the seismic velocities of methane gas hydrate-bearing sand, *Journal of Geophysical Research*, **10**, B04102, doi: 10.1029/2004JB003259.
22) Scholl, D. W. and Creager, J. S. (1973): Geologic synthesis of Leg-19 (DSDP) results; Far North Pacific and Aleutian Ridge and Bering Sea, *Internal Reports of the Deep Sea Drilling Project*, 897–913.
23) Shibuya, S. and Tanaka, H. (1996): Estimate of elastic shear modulus in Holocene soil deposits, *Soils and Foundations*, **36**(4), 45–55.
24) Shoji, H., Soloviev, V., Matoveeva, T., Mazurenko, L., Minami, H., Hachikubo, A., Hyakutake, K., Kaulio, V., Gladysch V., Logvina, E., Obzhirov, A., Baranov, B., Khlystov, O., Biebow, N., Poort, J., Jin, Y. K. and Kim, Y. (2005): Hydrate-bearing structures in the sea of Okhotsk, EOS, *American Geophysical Union*, **86**(40), 13–18.
25) Skempton, A. W. (1970): The consolidation of clays by gravitational compaction, *Geological Society*, **125**, 373–411.
26) Stoll, R. D., Ewing, J. I. and Bryan, G. M. (1971): Anomalous wave velocities in sediments containing gas hydrates, *Journal of Geophysical Research*, **76**, 2090–2094.
27) Wheeler, S. J. (1988): The undrained shear strength of soils containing large gas bubbles, *Gèotechnique*, **38**(3), 399–413.
28) Yamanaka, K. and Matsuo, K. (1962): Study of the soil hardness tester (1), *Journal of the Japan Society of Soil Science and Plant Nutrition*, **33**(4), 343–347 (in Japanese).
29) Yamashita, S. and Suzuki, T. (2001): Small strain stiffness on anisotropic consolidated state of sands by bender elements and cyclic loading tests, *Proc. 15th ICSMGE*, Istanbul, 325–328.
30) Yun, T. S., Narsilio, G. A. and Santamarina, J. C. (2006): Physical characterization of core samples recovered from Gulf of Mexico, *Marine and Petroleum Geology*, **23**, 893–900.
31) Zen, K., Yamazaki, H. and Umehara, Y. (1987): Experimental study on shear modulus and damping ratio of natural deposits for seismic response analysis, *Report of the Port and Harbour Research Institute*, **26**(1), 41–113.